2008 년 2 월

박사학위논문

Purification of amyloid beta peptide and mechanistic study of its interaction with biflavonoid inhibitors

조선대학교 대학원

생물신소재학과

Arjun Thapa

Purification of amyloid beta peptide and mechanistic study of its interaction with biflavonoid inhibitors

아밀로이드 베타의 정제와

프라보노이드와의 상호작용기전연구

2008 년 2 월 25 일

조선대학교 대학원

생물신소재학과

Arjun Thapa

Purification of amyloid beta peptide and mechanistic study of its interaction with biflavonoid inhibitors

지도교수 박 일 선

이 논문을 이학박사학위 논문으로 제출함

2007 년 10 월

조선대학교 대학원

생물신소재학과

Arjun Thapa

Arjun Thapa 의 박사학위논문을 인준함

위원장	조선대학교	교 수	함 경 수	인
위 원	조선대학교	교 수	박 일 선	인
위 원	연세대학교	교 수	조 병 연	인
위 원	조선대학교	교 수	신 송 엽	인
위 원	조선대학교	교 수	우 은 란	인

2007 년 12 월

조선대학교 대학원

CONTENTS

LIST OF TABLE……iv

LIST OF FIGURES……v

ABSTRACT……1

I. INTRODUCTION……3

I-1. Amyloid beta peptide……3

I-2. Purification of aggregation-prone proteins and peptides……4

I-3. Inhibition of amyloid beta toxicity……7

I-4. Outline of the thesis……10

II. MATERIALS AND METHODS……12

II-1. Materials……12

II-2. Identification of thermostable proteins from *E. coli*……13

II-3. Cloning of thermostable proteins……13

II-4. Expression and heat-stability of the prospective thermostable cloned genes……14

II-5. Construction of thermostable protein-ubiquitin-target fusion plasmid……15

II-6. Purification of Aβ42 and other targets……18

II-7. Circular dichroism spectroscopy……20

II-8. Cell culture and cell death assay……21

II-9. DEVDase and VDVADase assay……22

II-10. Preparation of Aβ solutions, Aβ42 oligomers and fibrils……23

II-11. Transmission electron microscopy……24

II-12. Western blotting……24

II-13. Thioflavin binding assay……25

II-14. Solubilization of RbsB-Aβ42 fusion protein……..27

III. RESULTS AND DISCUSSION……28

III-1. Soluble expression and purification of inclusion body-forming proteins and peptides……28

III-1.1. Identification of *E. coli* thermostable proteins.....28

III-1.2. Construction of plasmid vector with *E. coli* thermostable proteins……..……29

III-1.3. Application of plasmid vector for purification of other peptides……..……30

III-1.4. Application of plasmid vector for purification of proteins……..……32

III-2. Robust and specific inhibiting effects of dimeric flavones on Aβ induced toxicity……..……..39

III-2.1. Taiwaniaflavone potently inhibits Aβ induced Toxicity……..……..39

III-2.2. EM analysis of Aβ fibrillogenesis……..……40

III-2.3. TF accumulates non-toxic oligomers……..40

III-2.4. TF inhibits structural transformation of Aβ42……..……...43

III-2.5. TF potently inhibits polymerization, extension of Aβ42 fibers and preformed fibrils……..…….....44

III-2.6. Comparison of polymerization and extension kinetics of fibrillogenesis……46

III-2.7. Anti-amyloidogenic activity and cytoprotective effects of other related biflavonoids……..…….....47

III-3. Higher expression and stability of Aβ42 as fusion to D-ribose periplasmic protein……..……..62

III-3.1. Higher expression of RbsB-Aβ42 fusion protein…….62

III-3.2. Solubilization of RbsB-Aβ42 fusion protein……..…62
III-3.3. Application of RbsB fusion protein……..……63

IV. FURTHER STUDIES……..……66
IV.1. Inhibition of Aβ42 aggregation by β-sheet breaker Peptide……66

V. REFERENCES……..……68

VI. ACKNOWLEDGEMENTS……..……85

VII. ABBREVIATIONS……..……86

VIII. 적요……..……87

LIST OF TABLE

Table 1. IC_{50} of TF or other biflavonoids and biflavonoids……61

LIST OF FIGURES

Fig. 1. Identification and overexpression of thermostable *E. coli* proteins……..34
Fig. 2. Selection of fusion proteins for the vector Construction……..35
Fig. 3. Purification of Aβ42 and other peptides……...36
Fig. 4. Characterization of the purified peptides..……37
Fig. 5. Purification of reverse-caspase-2……..38
Fig. 6. Chemical structure of biflavonoids and other anti-amyloidogenic molecules….....51
Fig. 7 Effects of taiwaniaflavone and apigenin on cellular toxicity of Aβ42 or other toxic insults…….....52
Fig. 8. Effects of TF or AP on Aβ42 morphology 53
Fig. 9. Biochemical analysis Aβ42 fibrillogenesis……..54
Fig. 10. TF rescues cells exposed to Aβ42 oligomers and fibers.....55
Fig. 11. TF inhibits structural transformation of Aβ42……..56
Fig. 12. TF potently inhibits Aβ42 fibrillogenesis.....57
Fig. 13. AP partially inhibits Aβ42 fibrillogenesis……58
Fig. 14. Kinetic analysis of polymerization and extension kinetics of Aβ42.....59
Fig. 15. Effects of other related biflavonoids on Aβ42 induced toxicity and fibrillogenesis.....60
Fig. 16. Construction of RbsB fusion protein consisting vector and overexpression of Aβ42.....65
Fig. 17. Construction of recombinant Aβ42-GGVVIA fusion protein ……..67

ABSTRACT

Purification of amyloid beta and mechanistic study of its interaction with biflavonoid inhibitors

Arjun Thapa

Advisor: Prof. Il-Seon Park

Department of Biomaterials

Graduate School of Chosun University

Proteins and peptides expressed in the prokaryotic system often form inclusion body. Solubilization and refolding processes are required for their recovery but remain a tough task. In this study, an efficient plasmid vector system was constructed to purify those proteins and peptides in soluble form. The targets were expressed as a part of fusion protein and were cut off by cleavage at a specific site. To select a suitable fusion partner capable of solubilizing the aggregation-prone (inclusion-body forming) proteins and peptides, *Escherichia coli* thermostable proteins were screened and identified. Among them, trigger factor protein was selected for the following experiments because of its high expression and stability. Utilizing this system, Aβ and other selected protein and peptides that otherwise form inclusion body were expressed in soluble state and purified like other soluble proteins.

Proteins and peptides expressed in the prokaryotic system often form inclusion body. Solubilization and refolding processes are required for their recovery but remain a tough task. In this study, an efficient plasmid vector system was constructed to purify those proteins and peptides in soluble form. The targets were expressed as a part of fusion protein and were cut off by cleavage at a specific site. To select a suitable fusion partner capable of solubilizing the aggregation-prone (inclusion-body forming) proteins and peptides, *Escherichia coli* thermostable proteins were screened and identified. Among them, trigger factor protein was selected for the following experiments because of its high expression and stability. Utilizing this system, Aβ and other selected protein and peptides that otherwise form inclusion body were expressed in soluble state and purified like other soluble proteins.

I. INTRODUCTION

I-1. Amyloid beta peptide (Aβ)

Amyloid beta peptide (Aβ) is the causative agent of Alzheimer's disease (AD) [1]. Aβ peptides are produced by the sequential cleavage of transmembrane amyloid precursor protein (APP) by β and γ scretases [2-6]. The γ secretase, which produces C-terminal end of the Aβ peptide cleaves within the transmembrane region of the APP and subsequently generates several species of Aβ [3, 7, 8]. Aβ40 (40 amino acids long peptide) is typically produced by the cleavage that occurs in endoplasmic reticulum and Aβ42 in trans-Golgi network [7]. Aβ40 and Aβ42 are the most common forms of Aβ peptides found in AD brains. Aβ40 is more common form of the two; Aβ42 is highly fibrillogenic and associates with the disease states [9, 10]. Two additional hydrophobic residues at position Ile41 and Ala42 with greater propensities to transform into cross-β sheet structure are attributed to aggregating properties of Aβ42 relative to Aβ40 [11].

Small quantities of soluble monomeric form of Aβ peptides are present in cerebrospinal fluid and blood of healthy individuals [12]. Their levels are significantly increased with the progression of AD and deposits as fibrillar plaques [13, 14]. AD is clinically defined by the presence of extracellular senile plaques, intracellular neurofibrillary tangles and subsequent neuronal and synaptic loss [2, 15].

I-2. Purification of aggregation-prone proteins and peptides

Bacterial recombinant system is an ultimate choice for the production of large amounts of proteins or peptides required for the structural and biochemical studies when post-translational modification of the target is not essential [16]. *E. coli* remains the most efficient widely-used host for recombinant protein production. It facilitates protein expression by its relative simplicity, its inexpensive and fast high-density cultivation, the well-known genetics and the large number of compatible tools available for biotechnology [17]. However, poor expression, lower yield, instability of the target and difficulty in purification are inevitable complications [16, 18]. Furthermore, production of heterologous protein in *E. coli* often accumulates targets into insoluble aggregates known as inclusion body. Recovery of biological activity of the targets protein by *in vitro* refolding processes are tough task [19].

Inclusion body formation during heterologous protein expression is commonly observed due to lack of relevant interaction partners in host [17, 20]. In some cases, protein expression as inclusion bodies can be advantageous but their solubilization and renaturation processes are empirical and time-consuming [19]. The major obstacles are the poor recovery of the target and requirement for optimization of refolding conditions for each target. Renaturation procedure may also affect the integrity of refolded

proteins.

Maximizing the production of recombinant proteins in soluble form is therefore an attractive method compared to *in vitro* refolding procedures [17]. Under normal cellular conditions cytoplasmic proteins are able to fold spontaneously. But the aggregation-prone proteins require several molecular chaperones that interact reversibly with nascent polypeptide chains to prevent aggregation during folding [21]. Aggregation of recombinant proteins overexpressed in bacterial cells could result either from accumulation of high concentrations of folding intermediates or from inefficient processing by molecular chaperones [21, 22]. No universal method has been established for the efficient folding of aggregation-prone proteins and peptides.

Protein fusion technology is widely employed to improve expression, purification and solubility of recombinant protein expressed in *E. coli*. Several fusion proteins such as maltose binding protein (MBP) [23], thioredoxin (TRX) [24], transcription pausing factor L (NusA) [25], green fluorescent protein (GFP) [26], thiol-disulphide oxidoreductase (DsbA) [27], glutathione S-transferase (GST) [19], calmodulin binding protein [28], ubiqitin [18], small ubiquitin-related modifier (SUMO) are reported to enhance the solubility of fused protein. No systems and tools, however, appear to be the perfect choice for production of structurally diverse proteins. Although MBP is described as

an effective solubilizing agent compared to GST and TRX, it is unable to promote proper folding of non-native protein [23]. In many cases, it could not enhance the expression of difficult-to-express proteins [29, 30].

A major demerit of fusion protein is the covalent linkage of the two proteins, where presence of fusion partner may prevent or interfere with the subsequent use of desired protein. Truncated target proteins are reported from GST fusions and precipitation of membrane-bound viral protein (E8R) protein was observed after cleavage from its fusion partner, NusA [25]. Moreover, presence of linkers and extra amino acids may alter the biochemical properties of target. These common problems encountered in the fusion protein system clarifies that fusion partners have certain limitations. Several techniques have been exploited to increase the production of soluble proteins, for example, development of specific bacterial strains, chaperone co-expression and different cellular targeting [16, 25].

Stability of the fusion partner should be considered while purifying structurally diverse proteins [18, 25]. Recent reports described some thermostable proteins improve stability and purification process of targets fused to them [20, 31]. In this study, we examined several *E. coli* thermostable proteins capable of enhancing solubility of target proteins or peptides. Using the selected protein as a fusion partner, target protein and peptides that form

inclusion body in the conventional expression system were successfully expressed and purified without solubilization and any recovery processes.

I-3. Inhibition of Aβ cytotoxicity

Aβ peptide gradually transforms into the fibril via nucleation-dependent polymerization process [9]. During the process soluble Aβ oligomers and protofibrils are transiently formed, which may be intermediate to the fibril [32]. Neuronal impairment caused by Aβ peptide well correlates with the accumulation of the soluble, non-fibrillar forms, implying that they may be the main determinant in the occurrence of AD [10, 33]. Moreover, soluble oligomeric forms of Aβ is more cytotoxic than fibers [12, 34]. The mechanism leading to cell death resulting from Aβ fibrillogenesis is poorly understood. Several reports have linked Aβ toxicity with oxidative damage, ion and metal dyshomeostasis, mitochondrial dysfunction and apoptosis [35].

As no cure for AD is currently available, many efforts with several different strategies have been proposed to suppress the disease. Neutralization of Aβ by specific antibodies [36, 37], modulation of activity of either β or γ secretases [38, 39], and administration of anti-oxidant compounds [40], anti-inflammatory compounds, cholesterol-lowering drugs, Cu+2 and Zn+2 chelating agents [41] etc. are anticipated to reduce the AD

risks [35, 42]. These attempts, however, have never been efficient enough at the moment.

Therapeutic strategy targeting the Aβ fibrillogenesis is being practiced actively considering the fact that self-assembly of the peptide is a key factor involved in the pathogenesis of AD. For this reason, small molecules that efficiently inhibit the early steps of Aβ fibrillogenesis and stabilize the native non-toxic conformations are viewed as a solution to cure AD [43]. Curcumin [44], resveratrol [45], epigallocatechin gallate [46], and rosmarinic acid etc. are some of them. Curcumin, one of the most studied compounds, binds to the fibril-related conformation of Aβ peptide to reduce the amount of the oligomeric and protofibrillar forms [44]. The neuroprotective effect of the compound is associated with the reduction of toxic form of Aβ peptides although it displays free radical scavenging activities [44]. Anti-amyloidogenic activity of curcumin is comparable or even better than other small molecules like nordihydroguaiaretic acid (NGDA), chrysamine G, RS-0406 and congo red [44, 47, 48]

Small aromatic molecules are also aimed to stabilize Aβ aggregation [49, 50]. Vanillin, salicyclic acid and ferulic acid did not intervene the Aβ aggregation but the dimers of ferulic acid and benzothiazole derivatives are reported as therapeutics in dementia caused by the peptide [51]. This

indicates flat and planar molecules with more substituted aromatic groups can be Aβ ligand. Two terminal phenyl groups, aromatic substitutions that participate in hydrogen bonding, and optimal length and rigidity of the linker are regarded as important features of good inhibitors [52]. This hypothesis is further supported by the structural similarity of curcumin, congo red and RS0406 [44, 52].

On the other hand, diets rich in flavonoids are reported to lower the incidence of AD and other neurological disorders [40]. *Ginkgo biloba* extract EGb761 exhibited beneficial role in dementia and neuronal dysfunction associated with AD [53]. Flavonoid-free extract of *Ginkgo biloba*, HE208 failed to inhibit Aβ induced cellular toxicity, indicating that flavonoid component of the extract is essential for anti-amyloidogenic and anti-apoptotic effects [54]. Although the flavonoids have extensively been studied to develop AD drug [55, 56], their inhibitory mechanism regarding Aβ aggregation and cytotoxicity remains largely unclear. Myricetin, quercetin, kaempferol, morin, catechin and several other flavonoids are described anti-fibrillogenic and fibril-destablizing molecules but very few are cytoprotective [55-57]. The difference between myricetin and quercetin is a single OH group but the latter is unable to rescue cells exposed to Aβ in spite of its anti-fibrillogenic activities [58].

In this study, we examined the extract from *Selaginella tamariscina* to

isolate a small molecule that effectively and selectively inhibits the cell death induced by Aβ. As a result, taiwaniaflavone, dimeric form of apigenin, was purified. The “biflavone” was found to have strong anti-amyloidogenic and anti-cytotoxic effect, which was more specific and effective compared to its monomeric form. The findings demonstrate dimeric flavonoids could better neutralize deleterious effects of Aβ peptides.

I-4. Outline of the thesis

Initially purification of Aβ42 was focused in this study. Purification of homogeneous Aβ peptides is expected to be useful research materials in order to understand the possible mechanisms involved in the progression of yet unknown Alzheimer’s disease. The second portion of the thesis deals Aβ42 fibrillogenesis and its interaction with biflavonoids.

1. Several fusion proteins were screened for recombinant overexpression of the aggregation-prone peptide (Aβ42) in soluble state that otherwise forms inclusion bodies. Utilizing the stable fusion partner, an expression system was developed to easily purify Aβ42. The usage of the system is also examined by purifying misfolding prone proteins and other difficult peptides.

2. The selected fusion proteins were highly expressed and thermostable too. Only a few of them were considered worthy to make suitable fusion

partner for aggregation-prone proteins and peptides. One thermostable protein overexpressed Aβ42 in high amount and accumulated as inclusion body, which was solubilized and efficiently renatured.

3. Amyloidogenic activity of the Aβ42 is regarded as a key factor responsible for the pathogenesis of AD. Multiple mechanisms of Aβ toxicity and several ways to neutralize the action of Aβ have been described to cure AD. Biflavonoid molecules were employed to inhibit Aβ42 fibrillogenesis and cytotoxicity. Anti-amyloidogenic and cytoprotective effects of biflavonoids were compared to their monomeric form. In addition, recombinant Aβ42 fused to β-sheet breaker peptide was constructed to enhance solubility of the fusion protein and, hence attenuate cytotoxicity of the peptide.

II. MATERIALS AND METHODS

II-1. Materials

Acetonitrile was purchased from Merck. Dithiothreitol (DTT), ammonium hydroxide (NH_4OH), (4,5-dimethylthiazol-2yl) 2,5-diphenyl-tetarzolium bromide (MTT) and *N*,*N*-dimethylformamide (DMF) were from Sigma (St. Louis, USA). Caspase substrates (*N*-acetyl Val-Asp-Val-Ala-Asp-amino methyl coumarin [Ac-VDVAD-AMC]; *N*-acetyl Asp-Glu-Val-Asp-amino methyl coumarin [Ac-DEVD-AMC] were from A.G. Scientific Inc. (San Diego, USA). Cell culture reagents were from Welgene, Korea. Taiwaniaflavone (TF), 2',8" -biapigenin, amentoflavone, sumaflavone were isolated as previously described [59]. Apigenin (AP), thioflavin-T and dimethyl sulphoxide (DMSO) were purchased from Sigma (St. Louis, USA). Phosphate buffered saline (PBS) was from Amresco (Ohio, USA). ECL plus western blotting detection kit was obtained from Amersham Biosciences (Piscataway, USA). Monoclonal antibody (6E10) was acquired from Signet laboratories (Massachusetts, USA). All the other chemicals were obtained from Sigma (St. Louis, USA), unless otherwise specified.

II-2. Identification of thermostable proteins from *E. coli*

Whole cell lysate was prepared from *E. coli* DH5α cells by 4-5 passages through a French pressure cell at 18,000 lb/in^2 in lysis buffer (20 mM Tris-Cl [pH 8.0], 10 mM NaCl, 0.1 mM phenylmethanesulphonylfluoride, 0.1 mM EDTA and 1 mM β-mercaptoethanol) and centrifugation at 20,000 rpm for 1 h [16]. The soluble fraction (cell extract) was boiled for 10 min, centrifuged and the soluble fraction was again recovered. Proteins in the fraction were resolved in native 10% polyacrylamide gel electrophoresis (PAGE) [60]. Then, the gel portion containing protein was excised and denatured by boiling in the presence of 0.1% β-mercaptoethanol for 10 min followed by sodium dodecyl sulfate (SDS)-PAGE. The selected protein spots were analyzed by matrix-assisted laser desorption-ionization-time of flight (MALDI-TOF, Proteome Tech. Inc., Korea) and identified by NCBI blast search on the basis of probability.

II-3. Cloning of thermostable proteins

Genes encoding the identified thermostable proteins were PCR-amplified using *E. coli* DH5α genomic DNA as a template and cloned in *Nde*I and *Bam*HI sites (or *Nde*I/ *Hind*III for FK-506 binding protein, FKBP) of

pET21b expression system (Novagen). The primers used for cloning follows: DnaK (sense 5’-GAATTCCATATGGGTAAAATAATTGGTATC-3’, antisense 5’-GAAGAAGTCAAAGACAAAAAAGGATCCCG-3’); trigger factor (TiG, sense 5’-GGAATTCCATATGCAAGTTTCAGTTGAAAC-3’, antisense 5’-GAGCTGATGAACCAGCAGGCGGGATCCCG-3’); MBP (sense 5’-GGAATTCCATATGAAAATAAAAACAGGTG-3’, antisense 5’-CGCAGACTCGTATCACCAAGGTGGATCCCG-3’); D-ribose periplasmic protein (RbsB, sense 5’-GGAATTCCATATGAACATGAAAAAACTGGC-3’, antisense 5’-CTGAAACTGGTTGTTAAGCAGATGGATCCC-3’); putative EscN protein (EscN, sense 5’-GGAATTCCATATGACAACGTCAGACCGTCC-3’, antisense 5’-AAGTCCGCTCTATTCTTGATGCGGATCCCG-3’); GroES (sense 5’-GGAATTCCATATGAATATTCGTCCATTGCA-3’, antisense 5’-ATTCTGGCAATTGTTGAAGCGGGATCCGCG-3’); FKBP (sense 5’-GGAATTCCATATGAAATCACTGTTTAAAG-3, antisense 5’-CCGCAGATTCTGCTAAAAAAAAGCTTGGG-3’); Adenylate kinase (AKN, sense 5’-GGAATTCCATATGGTGGTATCGTTTATCG-3’, antisense 5’-GCTCTGGAAAAAATTCTCGGCGGATCCCG-3’); NusA (sense 5’-GGAATTCCATATGAACAAAGAAATTTTGGCTG-3’, antisense 5’-GCTGGTTCGGTGACGAAGCGTGGGATCCCG-3’).

II-4. Expression and heat-stability of the prospective thermostable cloned genes

Expression of proteins in *E. coli* BL21 (DE3) pLysS transformed with each gene was induced by 0.4 mM isopropyl-β-D-thiogalactopyranoside at ~ 0.6 of an OD_{600}, and was further cultured at 37 ºC for 4 h [16]. Cells were harvested, lysed in the lysis buffer (20 mM Tris-Cl [pH 8.0], 10 mM NaCl, 0.1 mM phenylmethanesulphonylfluoride, 0.1 mM EDTA and 1 mM β-mercaptoethanol), disrupted by a brief sonication and centrifuged at 16,000 x g for 1 h. SDS-PAGE analysis of the supernatant before and after boiling for 10 min was carried out to examine the expression and thermostability of the proteins.

II-5. Construction of thermostable protein-ubiquitin-target fusion plasmids

Aβ42 was PCR-amplified with primers (sense 5'-CGGGATCCAGATGAAGTTGATGATCGGAAATTTC-3', antisense 5'-CCGCTCGAGTCACGCAATCACCACGCCGCCCAC-3') using Aβ42 gene as a template and cloned in *Bam*HI and *Xho*I sites of pET28b plasmid (Novagen).

Ubiquitin gene (kindly provided by Rohan T. Baker) was cloned in *Nde*I/*Bam*HI sites before Aβ42 gene. Then, ubiquitin-Aβ42 was PCR-amplified (sense 5'-CGCGGATCCCAGATCTTTGTGAAGAC-3', antisense 5'-CCGCTCGAGTCACGCTATGACAACACCGCC-3') after removal of *Bam*HI site by site-directed mutagenesis (sense 5'-CTCCGCGGTGGAGATGCAGGATTC-3', antisense 5'-GGATCCTGCATCTCCACCGCGGAG-3') and cloned into *Bam*HI/*Xho*I sites in C-terminus of the selected thermostable proteins. Ubiquitin-Aβ40 construct was prepared by insertion of termination codon before two amino acid residues of Aβ42 sequence (sense 5'-GGGGGAGTATGAATCGCCCTC-3', antisense 5'-GAGGCCGATTCATACTCCCCC-3'). Using ubiquitin as a template, Aβ (42-1) was synthesized: (sense 5'-CGCGGATCCCAGATCTTTGTGAAGAC-3'; antisense1, 5'-CATCACGCCACCAACGACAATCGCTCCACCGCGGAGGCGCAAGAC-3'; antisense2, 5'-TGAGTTTTTACCTGCGATAATTCCGAGCATCACGCCACCAACGAC-3'; antisense3, 5'-CAACACGAAAAATGCTTCATCCACAACTGAGTTTTTAACTGCGAT-3'; antisense 4, 5'-TGATCCATATTCAACATGATGTTGTTTCAACACGAAAAATGCTTC-3';

antisense5, 5’-GAGTCAATCTGCTTCGAAGCGATGGTCTGATCCATATTCAACATG-3’; antisense6, 5’-CCGCTCGAGTCAATCTGCTTCGAA-3’) and subcloned after the TiG fusion protein. Humanin peptide [61] was synthesized by a sense primer (5’-CGCGGATCCCAGATCTTTGTGAAGAC-3’) and 3 antisense primers (5’-AAAACCACGCGGCGCCATTCCACCGCGGAGGCGCAA-3’, 5’-ATCAATTTCACCGGTCAGCAGCAGCAGGCAGCTAAAACCACGCGGCGCCAT-3’ and 5’-CCGCTCCAGTCACGCACGACGTTTCACCGGCAGATCAATTTCACCGGTCAG-3’) and subcloned as mentioned above. To construct reverse-caspase-2 [62], small and large subunit of the protein was PCR-amplified (primers for small subunit: sense 5’-GGATTCCATATGGCCGGTAAGAAAAGTTG-3’ and antisense 5’-CGGATCCTGTGGGAGGGTGTCCTGG-3’; primers for large subunit: sense 5’-CGGATCCGGTCCTGTCTGCCTTCAAG-3’ and antisense 5’-GCGTTTTTTGCGGCCATCTTGTTGGTCAACCCC-3’). Small subunit of the full length caspase-2 was cloned in pET21b following the large subunit. Finally, the whole structure was subcloned into *Bam*HI/*Xho*I sites of the newly constructed TiG-ubiquitin plasmid. The plasmid was constructed by PCR-amplification with primers (sense 5’-GAATTCCATATGCAAGTTTCAGTTGAAAC-3’, antisense 5’-

CGCGGATCCACCGCGGAGGCGCAACAACAG-3') cloned into *Nde*I/*Bam*HI of pET21b expression system, after removing *Bam*HI site linking TiG and ubiquitin. In addition, pGEX-Aβ42 construct was digested by *Bam*HI and *Xho*I and the resulting insert was subcloned after candidate thermostable protein (RbsB). Site directed mutagenesis using (sense-5'-AAGCAGATGGGATTCGATGCAG-3'; antisense 5'-CTGCATCGGATCCCATCTGCTT-3') was carried out to generate inframe cloned RbsB-Aβ42 expressing plasmids.

II-6. Purification of Aβ42 and other targets

Aβ42 as fusion to TiG and ubiqitin was overexpressed and the cell extract was prepared as described above. Soluble fraction was applied to Ni-NTA column (Amersham Biosciences), washed with 5 column volumes of buffer A (50 mM Tris-Cl [pH 8.0], 150 mM NaCl, and 1 mM β-mercaptoethanol) and protein was eluted with buffer B (buffer A + 250 mM imidazole). Peak fractions of the fusion protein were pooled, quantified, two-fold diluted and incubated with Usp-2cc [18] in 1:100 enzyme-protein molar ratio at 37 ℃ for 2 h. The samples were then subje cted to preparative RP-HPLC (C_{18} column, 25 mm x 250 mm x 8 μm, Grace Vydac). Aβ42 was

purified with a solvent system buffer C (30 mM ammonium acetate [pH 10.0] and 2% acetonitrile) and buffer D (70% acetonitrile in water) at a flow rate 10 ml/min using a 20-40% linear gradient of buffer D over 35 min. The same protocol was used for purification of Aβ40 and Aβ (42-1). Humanin [61] was purified in silica based column, with buffer E (0.1% TFA in water) and buffer F (buffer E + 80% acetonitrile), using a 5-60% linear gradient of buffer F over 40 min. Purified peptides were lyophilized and stored at -20 ºC. Immediately before use, the peptides Aβ40, Aβ42 and Aβ (42-1) were dissolved in 0.1% NH_4OH [63] at a concentration of 2 mg/ml, followed by bath sonication for 10 min and resuspended in PBS (10 mM phosphate buffer [pH 7.4], 137 mM NaCl, and 2 mM KCl). Humanin was dissolved in 10% glacial acetic acid and subsequently diluted 5 times in PBS.

For reverse-caspase-2 [62], TiG-ubiquitin-reverse-caspase-2 was overexpressed for 4 h at 30 ºC with 0.4 mM IPTG. Cells were lysed in lysis buffer B (20 mM Tris-Cl [pH 8.0], 10 mM NaCl, and 0.1 mM EDTA and 1 mM β-mercaptoethanol), disrupted by French pressure cell and centrifuged at 20,000 rpm for 1 h. Cell extract was injected into Ni-NTA column, washed 5 column volumes of buffer G (20 mM Tris-Cl [pH 8.0], 10 mM NaCl, and 1 mM β-mercaptoethanol) and eluted by linear gradient of buffer H (buffer G + 250 mM imidazole). The two-fold diluted fusion protein fractions were digested by

the Usp2-cc enzyme and purified by HiTrap Q column (Amersham Biosciences) chromatography using buffer I (20 mM Hepes-NaOH, [pH 7.5], 10 mM NaCl, 0.1 mM EDTA, 10% glycerol and 1 mM DTT) and buffer J (buffer I + 1 M NaCl). Pooled fractions were dialyzed to remove NaCl and loaded in HiTrap CM column (Amersham Biosciences) for final purification step. Buffer K (20 mM Hepes-NaOH, [pH 7.0], 10 mM NaCl, 0.1 mM EDTA, 10% glycerol and 1 mM DTT) was used as washing buffer and the proteins were eluted with buffer L (buffer K + 1 M NaCl). The purified enzymes were dialyzed in buffer K + 10 mM NaCl and stored at –80 ºC.

II-7. Circular dichroism spectroscopy

Aβ42 (20 μM) was incubated in PBS at 37 °C either alone or presence of TF (20 μM) or AP (20 μM) for 0, 12 or 24 h. CD spectra [64] were recorded with a 1-mm path length cuvette at 0.5 nm intervals between 190 nm and 250 nm at 1 nm resolution with a scan rate of 50 nm/min using a Jasco Sectropolarimeter (Jasco Co., Tokyo, Japan) at 25 °C. Five scans were recorded and averaged for each sample. Aβ spectra were obtained by subtracting buffer background (PBS containing 0.2% DMSO and 0.004% NH_4OH). Background spectra given by alone TF or AP in identical conditions

were subtracted from Aβ samples incubated in presence of TF or AP. The corrected, averaged spectra were smoothed using means-movement algorithm in Jasco spectra analysis program.

II-8. Cell culture and cell death assay

Human neuroblastoma SH-SY5Y cells were cultured in Dulbecco's Modified Eagles medium and Ham's F 12 (1:1) supplemented with 10% (v/v) fetal bovine serum (FBS) and 1% antibiotics at 37 °C under 5% CO_2. Cells were seeded at a density of 15,000 cells/well in 96-well plates (Nunc, Denmark) and incubated for 24 h. The cells were replaced with serum-free media and cells were further cultured for 12 h [44, 65]. To test the biological activity of the purified peptides, Aβ40 or Aβ42, cells were treated with indicated concentrations of peptides for 24 h. Cell viability was assessed by MTT reduction assay [66, 67]. Briefly, 20 μl of 5 mg/ml MTT solution in PBS was added to each well and incubated. After 2 h, 100 μl of solubilization buffer [20% SDS solution in 50% (v/v) DMF (pH 4.7)] was added. The absorbance was recorded after 12-16 h using microplate reader on Spectra Max 190 (Molecular Devices, CA, USA) at 570 nm. For other experiments, cells were treated with Aβ42 (0.5 μM) or other cytotoxic insults staurosporine (25 nM),

brefildin A (1 μM), etoposide (1 μM) in presence varying concentrations of taiwaniaflavone (TF) or apigenin (AP) as indicated. Aβ peptides and other chemicals were further diluted in culture media maintaining ~0.2% DMSO.

II-9. DEVDase and VDVADase assays

To measure DEVDase (caspase-3/7-like) activity [65], Aβ40 (20 μM) or Aβ42 (20 μM) treated cells were washed twice with ice-cold PBS. Then, 40 μl of cell lysis buffer (20 mM Hepes-NaOH [pH 7.0], 1 mM EDTA, 1 mM EGTA, 20 mM NaCl, 1 mM DTT, 1 mM phenylmethanesulphonylfluoride, 10 μg/ml leupeptin, 5 μg/ml pepstatin A, 2 μg/ml aprotinin, 25 μg/ml ALLN) was added into each well and incubated on ice for 20 min. The enzyme activity assay was performed with the addition of 60 μl caspase assay buffer (10 mM Hepes-KOH [pH 7.0], 10 mM NaCl, 1.5 mM $MgCl_2$, 1 mM EDTA, 1 mM EGTA and 10 mM DTT) including 10 μM DEVD-AMC (substrate). Enzymatic activity of reverse-caspase-2 was examined using 10 μM Ac-VDVAD-AMC. The activity was monitored at an excitation and emission wavelengths of 360 nm and 480 nm respectively, using micro plate spectrofluoremeter (Molecular Devices, CA, USA). For rest experiment, cells were treated with Aβ42 (0.5 μM) or STS (25 nM) in presence of varying concentrations of TF or AP for 12 h. DEVDase

activity was determined described as above.

II-10. Preparation of Aβ solutions, Aβ42 oligomers and fibrils

Purified Aβ40 and Aβ42 peptides were monomerized in HFIP [68], dried under nitrogen flow, speed vacuumed for 30 min and stored at –20 °C. Before use, the peptides were dissolved in 0.1% NH_4OH at a concentration of 2 mg/ml followed by bath sonication for 10 min [63], and then solutions were mixed with an equal volume of PBS (10 mM phosphate buffer, pH 7.4, 137 mM NaCl, and 2 mM KCl). To make Aβ42 oligomers [32, 33], peptides were diluted in cell culture media at (1 μM) concentration, vortexed for 30 seconds and incubated at 4 °C for 24 h [63]. The reaction mixture was centrifuged at 16000 x g for 15 min. No visible pellet was observed after centrifugation. Fibrils were prepared at high concentration of the peptide. Aβ42 (100 μM) was incubated in presence of 0.02% sodium azide in PBS at 37 °C for 4 days. The samples were centrifuged at 16000 x g for 30 min. Pellet fraction (fibrils) was washed three times with PBS. Fibrils were sonicated for 10 min, quantified by Bradford method and used immediately or stored at –80 °C.

II-11. Transmission electron microscopy

Aβ42 (0.5 μM) either alone or in presence TF or AP was incubated in PBS at 37 ℃ for 12 h. Final concentration of DMSO was maintained ~0.2% in the reactions. A 5 μl of sample was adsorbed on Formvar-coated 200-mesh nickel grids for 15 min and air-dried overnight [69]. The grids were negatively stained with 2% uranyl acetate for 1 min, washed with distilled water for at least three times. The samples were then analyzed with transmission electron microscopy (Hitachi, Japan) at an accelerating voltage of 80 kV at magnification of 40,000x.

II-12. Western blotting

Aβ42 (0.5 μM) in presence of TF or AP was incubated in PBS at 37 ℃ for 12 h. The incubated reaction mixtures were crosslinked [70]. Briefly, a final concentration of glutaraldehyde (0.01%) was added to the reaction for 5 min and the reaction was terminated with 2 x SDS sample buffer (50 mM Tris pH 6.8, 10% glycerol, 2% SDS, and 0.1% β-mercaptoethanol). Samples were separated on 16% sodium dodecylsulphate-polyacrylamide gel electrophoresis (SDS-PAGE) and transferred to polyvinylidene difluoride membrane (Bio-rad laboratories, Hercules, USA). Blots were blocked in 5% milk in Tris-buffered saline containing 0.2% Tween 20 at room temperature for

1 h. The membranes were probed with primary monoclonal antibody to Aβ (6E10) and anti-mouse horseradish peroxidase-conjugated secondary antibodies. The blots were visualized using ECL plus reagent kit.

II-13. Thioflavin-T binding assay

To test the amyloidogenic property of the purified peptide, Aβ42 (20 μM) or Aβ40 (40 μM) was incubated in PBS at 37 ℃ for indica ted time period. Fibrillogenesis study was performed at 37 ℃ using the thioflavin-T dye and release of fluorescence was monitored at an excitation and emission wavelength of 445 and 490 nm respectively [58, 71], using micro plate spectrofluoremeter (Molecular Devices, CA, USA). A 20 μl of reaction mixture was mixed with 80 μl of 5 μM thioflavin-T in PBS at indicated time point and fluorescence was measured. For polymerization assay, Aβ42 (20 μM) was incubated in PBS at 37 °C in presence of TF (0-16 μM) or AP (0-40 μM) μM in a final volume of 300 μl without shaking. Thioflavin-T fluorescence representing the characteristic sigmoidal curve was plotted as common logarithms in equation $\log\left[F(t)/A - F(t)\right] = at + b$ where t is the reaction time, $F(t)$ is the fluorescence as a function of time, A is tentatively determined as $F(\infty)$, and a and b are the slope

and $y-$ intercept, respectively. Differentiating above equation by t and subsequent rearrangement produced a logistic equation, $F'(t) = BF(t)[A - F(t)]$, where, $B = a \ln 10\, A/2$, and $F'(t)$ represents rate of fluorescence increase at a given time. When $F(t) = A/2$, $F(t)/A - F(t) = 1$ and $F'(t)$ reaches its maximum. This time point was referred as $t/2$ [72]. For Aβ42 fiber extension assay, fresh Aβ42 (20 μM) was incubated with preformed Aβ42 fibril (1.1 μM) in presence of varying concentration of TF or AP. For fiber destabilization assay, preformed Aβ42 fiber (20 μM) was incubated in presence of varying concentration of TF (0-20 μM) or AP (0-40 μM). RFU without compound was regarded as (100%) and IC_{50} (concentrations required to inhibit the fibrillogenesis by 50%) was calculated by plotting fluorescence (%) versus concentrations of TF or AP in log (μM) as described earlier [58].

Aβ42 fibrillogenesis assay was also performed at low concentration of Aβ42. In this case, Aβ42 (0.5 μM) was incubated in a final volume of 200 μl in presence of (0, 5 and 10 μM) of 2',8''-biapigenin or amentoflavone or sumaflavone for 0, 3, 6 and 12 h. A 180 μl of reaction mixture was mixed with 20 μl of thioflavin-T (50 μM). RFU was determined by subtracting buffer background (PBS containing 0.2% DMSO and 0.004% NH_4OH).

II-14. Solubilization of RbsB-Aβ42 of fusion protein

Aβ42 as fusion to RbsB [73] was overexpressed essentially as described before. Inclusion bodies were washed 3 times with 20 ml (for 1 liter culture) buffer M (50 mM Tris-Cl pH 8.0, 150 mM NaCl, 0.1 mM EDTA) by centrifuging at 16000 rpm for 20 min. Intact fusion protein was solubilized in 20 ml buffer N (50 mM Tris-Cl pH 8.0, 150 mM NaCl, 6 M urea, and 1 mM DTT), clarified by centrifugation at 16000 rpm for 1 h and dialyzed [74]. Purity and molecular weight of the proteins were judged by SDS-PAGE analysis, quantified by Bradford method and stored at 4 ºC.

III. RESULTS AND DISCUSSION

III-1. Soluble expression and purification of inclusion-body forming peptides and protein by fusion to *Escherichia coli* thermostable proteins

III-1.1 Identification of *E. coli* thermostable proteins

Many proteins and peptides expressed in *E. coli* form insoluble inclusion body. Although it has some advantages in the purification, solubilization and recovery of biological activity of the targets persist as problems [75]. Fusion of the target proteins or peptides to a protein that makes them soluble might be a way to solve these difficulties. It is speculated that highly soluble and stable protein could assist the proper folding and solubilization of heterologous target [20, 22] and thermostable proteins [31] might have the capability. According to the speculation we examined the several indigenous *E. coli* thermostable proteins if they could make aggregation-prone peptides and proteins soluble.

To isolate thermostable proteins from *E. coli* proteome, the cell extract was boiled for 10 min and the soluble fraction was saved after extensive

centrifugation. About 15 proteins in the fraction could be identified by PAGE and subsequent MALDI-TOF analysis (Fig. 1A). Among the candidates, genes encoding ten proteins selected arbitrarily were cloned, expressed and analyzed for the overexpression and thermostability. DnaK, NusA, TiG, FKBP, AKN, GroES and EscN proteins [22, 76-78] were highly expressed and thermostable, whereas some part of MBP precipitated upon boiling although it expressed well (Fig. 1B). RbsB [73] was also highly expressed but two bands were observed by an unknown reason. On the other hand, ribosomal protein SS19 was poorly expressed (Fig. 1B). After exclusion of some proteins that were not expressed well or already tested before [25], DnaK, TiG, FKBP, AKN, EscN and MBP proteins were selected for the following experiments.

III-1.2 Construction of plasmid vector with *E. coli* thermostable proteins

Aβ42 peptide was chosen as an initial target because the peptide was previously reported to form the inclusion body in *E. coli* and was purified from it [74, 79]. A plasmid vector was designed and constructed to contain the selected proteins, ubiquitin to specifically cut off the target from the fusion protein by a deubiquitylating enzyme, Usp2-cc [18] and Aβ42 (Fig. 2A). Each

construct with the selected thermostable proteins was expressed in *E. coli* and examined for expression and solubility. DnaK and TiG fusions were highly soluble, whereas the large portion (>70%) of EscN fusion was found as the inclusion body (Fig. 2B). MBP was described in other studies as a choice of the fusion partner for promoting the solubility of the fused polypeptides but its fusion with Aβ42 was largely insoluble (Fig. 2B). While FKBP and AKN fusion proteins were not expressed by unknown reason (data not shown). DnaK, an ATP-dependent molecular chaperonin working with other co-chaperonins and highly expressed in *E. coli*, was not preferred for the purpose [76]. Rather, relatively smaller TiG, acting in nascent polypeptide chain [77], was finally utilized as a fusion partner (Fig. 2A and B).

III-1.3 Application of the plasmid vector for purification of other peptides

TiG-ubiquitin-Aβ42 fusion protein was stable at 4 °C over a month. The initial purification through Ni-NTA column chromatography was followed by treatment of the fractions by Usp-2cc to cut off the peptide (Fig. 3A). Then the digested fractions were subjected to the conventional C_{18} column chromatography (Fig. 3A and B). Aβ42 eluted as a single peak (Fig. 3B) and

was homogeneous in PAGE (Fig. 3A, lane 3) and MALDI-TOF MS analysis (measure mass, 4514.6 Da; expected value, 4513.8 Da; data not shown). About 6 mg of the peptide per liter bacterial culture could be obtained, which is approximately 1.5 times better, compared to other result [74]. Using this system, Aβ40, Aβ (42-1) (a reverse form of Aβ42) and humanin (24 amino acids long peptide) were also successfully purified and the yield was comparable (~ 8, ~ 6 and ~ 8 mg from one liter bacterial culture, respectively) (Fig. 3C).

The biophysical and biochemical characteristics of amyloid peptide depend upon how it is produced or prepared [80, 81]. The purified Aβ42 and Aβ40 peptides were examined if they have the characteristics reported previously. The typical curves of fibrillogenesis (Fig. 4A) were observed for both Aβ42 and Aβ40 by thioflavin T binding assay, which was consistent with previous report [71]. In CD spectroscopy, predominant the random coil conformation of freshly dissolved Aβ42 and β-sheet structure of the aggregated peptide were observed (Fig. 4B), indicating that the biophysical properties of the purified peptides were preserved [64]. Furthermore, cellular toxicity of the two peptides (Fig. 4C) with increase of caspase-3 activity (Fig. 4D) in human neuroblastoma SH-SY5Y cells confirmed that the purified peptides were biologically functional.

III-1.4 Application of the plasmid vector for protein purification

The plasmid vector system was also applied for purification of a protein that formed the inclusion body when expressed in *E. coli*. We had a difficulty in producing reverse form of caspase-2 (reverse-caspase-2) where the small subunit was followed by the large subunit to make it constitutively active without processing [62]. The enzyme accumulated as the inclusion body in the conventional *E. coli* expression system (Fig. 5A). Trials to recover soluble and active enzyme from the inclusion body by solubilization in urea and refolding by dialysis were unsuccessful in that only small amount of soluble protein was obtained and it was even catalytically inactive. Therefore, TiG-ubiquitin-reverse-caspase-2 was constructed using the vector system to solve the problem. The fusion protein was successfully expressed at a high level in a soluble form (Fig. 5B) and was purified without the difficulty by the method as described in materials and method (Fig. 5C). About 0.3 mg of active reverse-caspase-2 was obtained from one liter bacterial culture. The purified enzyme had activity comparable to that of normal caspase-2 which is usually recovered in the soluble fraction by the conventional purification system (Fig. 5D), indicated that the biochemical characteristics of the protein purified by this system are unaltered.

In summary, a plasmid vector was developed using TiG as a fusion partner to produce and recover aggregation-prone peptides and protein in soluble state. The easy purification steps, specific cleavage of the fusion protein and satisfactory yields give it the advantage of being a tool for production of proteins and peptides that form the inclusion body in *E. coli*.

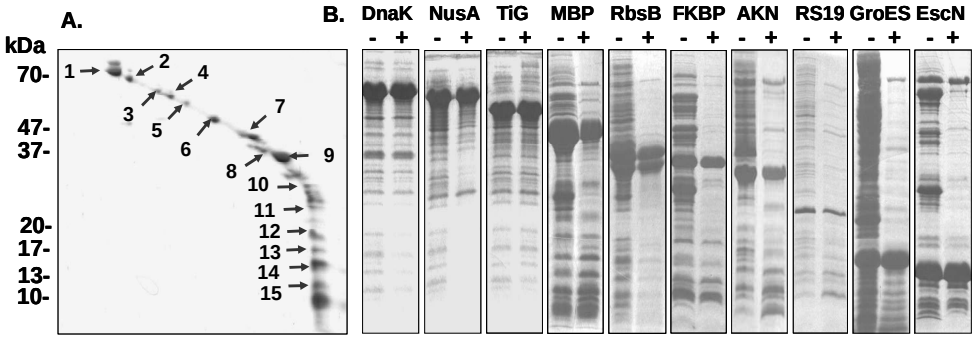

Fig. 1. Identification and overexpression of thermostable *E. coli* proteins.

(A) Two-dimensional PAGE analysis of thermostable *E. coli* proteins. Cell extract was boiled for 10 min and the supernatant after centrifugation was saved. The native gel portion containing the supernatant was excised, denatured and subjected to SDS-PAGE. The indicated spots were identified by MALDI-TOF as follows: 1, DnaK; 2, NusA; 3, 4, 5, TiG; 6, MBP; 7, galactose glucose binding protein; 8, FKBP; 9, RbsB; 10, AKN; 11, outer membrane lipoprotein carrier protein; 12, 50S ribosomal protein S19 (RS19); 13, EscN; 14, GroES; and 15, ribosomal protein SS19. Relative molecular weights are indicated on the left. **(B)** SDS-PAGE analysis of the selected proteins that were overexpressed in *E. coli*. For TiG spot 5 was used. Each pair of lanes consists of the equivalent amount of protein before (-) and after (+) boiling. MBP, FKBP, AKN, RS19, and EscN proteins were loaded ten times as much as others.

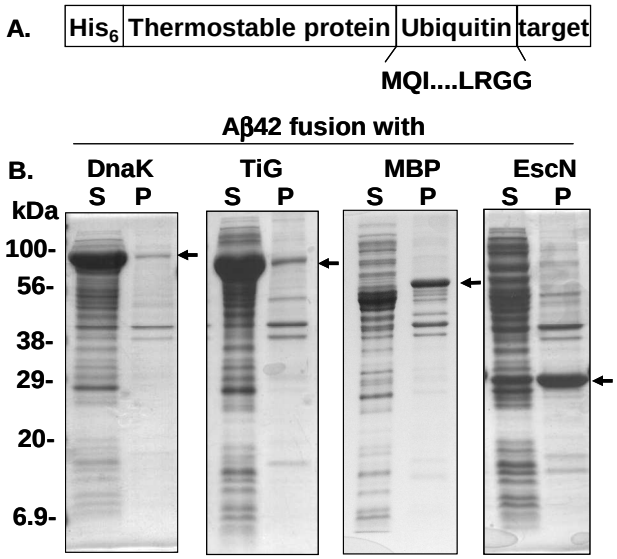

Fig. 2. Selection of fusion protein for the vector construction. (A) Schematic representation of the construct used for soluble expression of target protein (not drawn to scale). Parts of amino acid sequences of ubiquitin are indicated. **(B)** SDS-PAGE analysis of the selected fusion proteins. The cell extract from each construct was centrifuged and soluble (S) and insoluble (P) fractions were analyzed by SDS-PAGE to examine if they confer solubility to Aβ42 on the fusion. An equal amount of soluble and insoluble fractions was loaded in each pair of lanes. The arrows indicate the overexpressed fusion proteins. Relative molecular weights are indicated on the left.

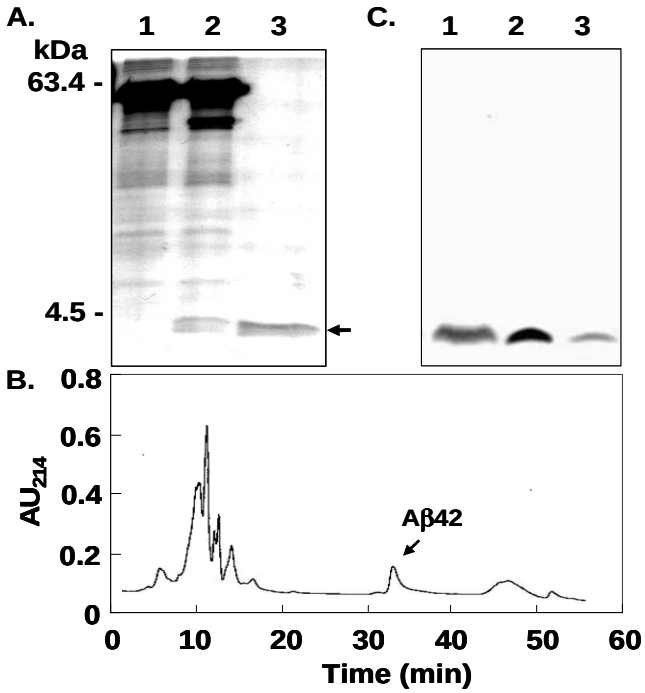

Fig. 3. Purification of Aβ42 and other peptides. (A) Tricine PAGE (polyacrylamide: 13.5%) analysis of Aβ42 and its fusion protein. Lanes: 1, TiG-ubiquitin-Aβ42 fusion protein purified using Ni-NTA column; 2, the fusion protein digested by Usp2-cc; 3, Aβ42 purified by C_{18} reverse phase column chromatography.**(B)** Aβ42 elution profile of C_{18} reverse phase column chromatography. **(C)** Tricine PAGE analysis of Aβ42 (lane-1), Aβ40 (lane-2) and humanin (lane-3) fractions. The peptides were overexpressed and purified by the same method as Aβ42 using TiG-based vector construct as described. Arrows in **(A)** and **(C)** indicate the purified peptides.

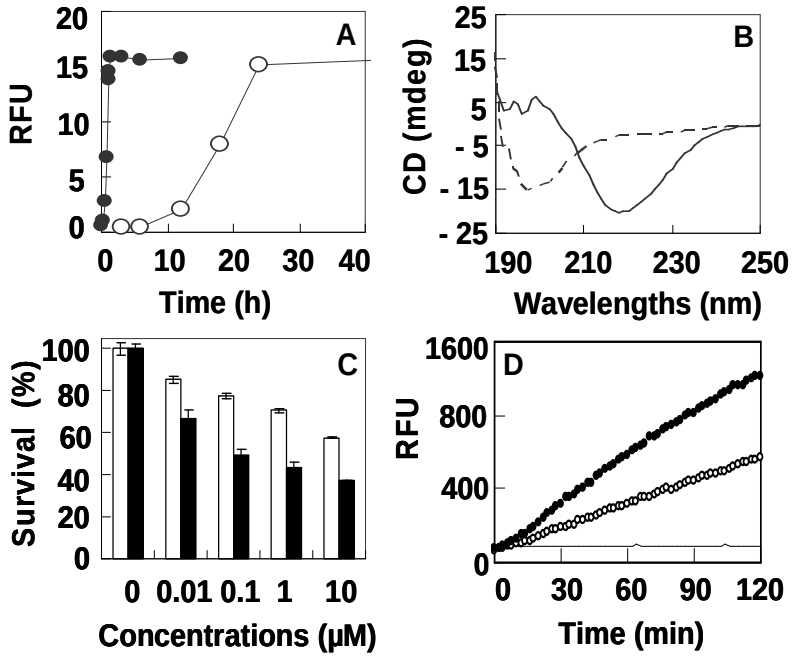

Fig. 4. Characterization of purified peptides. The purified Aβ peptides were tested for their biophysical and biochemical properties. **(A)** Time-dependent fibrillogenesis curve of Aβ42 (close circle) and Aβ40 (open circle) obtained by thioflavin T binding assay. **(B)** CD spectra showing random coil conformation of freshly dissolved Aβ42 (broken line) and β-sheet structure when aggregated for 24 h (solid line). **(C)** MTT assay showing dose-dependent toxicity of Aβ42 (close bar) and Aβ40 (open bar) in SH-SY5Y cells. **(D)** DEVDase activity analysis in cells exposed to 20 μM Aβ42 (close circle) and 20 μM Aβ40 (open circle) or in untreated cells (thin line) with 10 μM DEVD-AMC as a substrate. RFU: relative fluorescence unit.

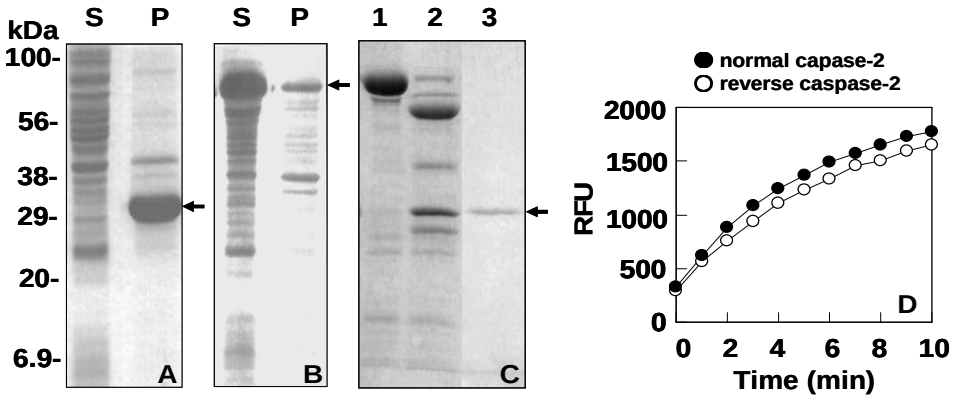

Fig. 5. Purification of reverse-caspase-2. (A) SDS-PAGE analysis of reverse-caspase-2 in the cell extract. S and P represent the soluble and insoluble fractions of the overexpressed protein. Relative molecular weights are indicated on the left. **(B)** SDS-PAGE analysis of TiG-ubiquitin-revese-caspase-2 in the cell extract. **(C)** SDS-PAGE analysis of TiG-ubiquitin-revese-caspase-2 purified by Ni-NTA column chromatography (lane-1), the fusion protein digested by Usp2-cc (lane-2), and reverse-caspase-2 purified (lane-3) by CM column chromatography. Arrowheads in panel **(A)**, **(B)** and **(C)** indicate position of insoluble reverse-caspase-2, soluble TiG-ubiquitin-reverse-caspase-2 and purified reverse-caspase-2, respectively. **(D)** VDVADase activity analysis of purified reverse-caspase-2 (100 ng, open circle) and the normal caspase-2 (100 ng, closed circle) with 10 μM VDVAD-AMC as a substrate.

III-2. Robust and specific inhibiting effect of dimeric flavones on β-amyloid cytotoxicity and fibrillogenesis than its monomoric form

III-2.1 Taiwaniaflavone potently inhibits Aβ induced toxicity

Multiple mechanisms and broad spectrum biological effects of flavonoids are suggested to be associated with their neuroprotective action [65]. Here, biological activity of dimeric flavone (taiwaniaflavone, TF) (Fig. 6) and monomeric flavone [46] (apigenin, AP) was compared against various cellular insults such as staurosporine (DNA damage), brefildin A (endoplasmic reticulum stress), etoposide (mitochondrial damage) and Aβ42 on cultured SH-SY5Y cells. TF potently inhibited cell death induced by Aβ. It also showed some effect in STS but not in BFA and ETO induced cell death (Fig. 7A). In contrast, AP attenuated the Aβ induced cell death less effectively but it was effective in other insults tested here (Fig. 7A). Cell viability was assessed by MTT assay. Aβ42 (0.5 μM) alone caused ~50% cell death in 12 h under our experimental condition and this concentration was maintained for all experiments as far as possible. Considering the fact that aggregated Aβ is less toxic [82], preincubation of Aβ either alone or in presence of chemicals

was avoided.

Caspase assays were performed to measure caspase-3/7 like activity of the cells committing death. Lower caspase activity was observed in Aβ treated cells under the described condition (Fig. 7B), revealing that higher concentration of Aβ and longer exposure times are required to see greater effect [83]. On the other hand, higher caspase activity was observed in STS treated cells. AP potently inhibited activation of caspase-3 in STS induced cell death (Fig. 7B), indicating that the involvement of AP in other cellular survival events [57]. To examine interaction TF or AP on exogenously added Aβ, cells were preincubated with the chemicals for 12 h and treated with Aβ (0.5 μM) later. As expected both of these chemicals were ineffective (Fig. 7C). It suggests that the activity of TF or AP was the direct consequence of interaction with Aβ. Altogether, these observations suggest TF potently inhibits Aβ toxicity. Inhibitory concentration to rescue the cell death by 50% was found to be ~1 μM.

III-2.2 Electron microscopic analysis of Aβ fibrillogenesis

Aggregation states of self-associating Aβ peptides are associated with toxicity [67]. To determine whether cytoprotective effect of TF or AP is linked

to inhibit Aβ fibrillogenesis, Aβ aggregates formed in the identical condition as in cell culture with or without TF or AP was visualized by EM. Aβ alone showed heterogeneous population of oligomers ranging 3-10 nm, beaded protofibrillar structures < 200 nm and immature fibers (Fig. 8) as described in earlier study [67]. Inspection of large number of fields failed to reveal mature fiber [51] in the described condition, suggesting that cell death was the result of the oligomers and protofibrils. In the presence of TF, protobrillar structures were not found but spherical particles, small oligomers, occasionally amorphous deposits were seen although fewer in number (Fig. 8). The presence of earliest species of Aβ fibrillogenesis such as dimers, trimers, small oligomers and Aβ-derived diffusible ligands (ADDLs) can be speculated if the fibrillogenesis is arrested at early phase. Relatively large oligomers were predominant species in presence of AP (Fig. 8). Potent inhibition of Aβ fibrillogenesis by TF was visually evident and it also suggested TF interacts with Aβ and prevent their growth. This unusual visualization of oligomeric species in presence of TF desired further investigations to prove their existence.

III-2.3 TF accumulates non-toxic oligomers

The above result indicated cytoprotective effect of TF despite the accumulation of oligomers. Western blot analysis was performed to define the Aβ species visualized by EM. Samples were prepared essentially as in EM analysis and crosslinked [70]. Many species of Aβ including trimers, tetramers and oligomers could be induced in gel or degrade upon boiling [84]. Aggregation reaction was crosslinked to show all the possible species of Aβ that are either simply not observed in gel or susceptible to induction or degradation during separation. High molecular weight species of Aβ ~100 kDa were observed after 3 h incubation (Fig. 9A). Monomeric Aβ disappeared and completely become aggregated after 12 h (Fig. 9B). In the presence of TF, relative density of the Aβ monomer was not reduced even after 12 h and those predominant species observed at early time point (3 h) remained as such (Fig. 9A and B). It suggested that TF bound to oligomers formed at earlier time points and prevented their further polymerization (Fig. 9A). This result is consistent with the previous work, which shows accumulation Aβ dimers and oligomers in presence of polyphenolic inhibitors [85]. In presence of AP, Aβ monomers decreased with the promotion of large oligomers (Fig. 9B). Crosslinked aggregated Aβ showed high molecular weight single band (Fig. 9B) whereas the oligomers separated as a smear [84], possibly providing greater surface area to interact the anti-bodies. Their actual amount is likely to

be much less than observed in gel (Fig. 9 A and B).

Aβ oligomers are the most toxic species known so far [33]. Aβ oligomers were isolated to study effect of TF or AP on enriched Aβ oligomers. Isolated Aβ oligomers were similar to the oligomers described in previous reports [10, 33]. Virtually no difference was observed in oligomeric preparation Aβ before and after centrifugation (Fig. 10A). Crosslinked oligomeric preparation of Aβ demonstrated several species of Aβ (Fig. 10A, lane-4). Aβ42 oligomers (supernatant fraction) caused ~15% more cell death in 12 h compared to fresh Aβ42. TF was effective against Aβ oligomers as well as fibers but not AP (Fig. 10B and C). These results suggest that TF could detoxify the effect of several distinguished species of Aβ formed during or at the end of fibrillogenesis.

III-2.4 TF inhibits structural transformation of Aβ42

Aβ fibrillogenesis is accompanied by the gradual structural transition of the peptide into β-sheet structure [64]. CD spectroscopy revealed that freshly dissolved Aβ42 (20 μM) adopted random coil conformation displaying negative signal at 195 nm but upon incubation transformed into β-sheet conformation (reached the maximum at 12 h), showing more negative

ellipticity around 216 nm (Fig. 11A and B). In the presence of TF (20 μM), CD spectrum was dominated by random coil-like shape (Fig. 11A), suggesting that TF inhibits conformational change of the peptide. This result completely agrees with the previous analysis of secondary structures of Aβ42 in presence of myricetin [86] and β-cyclodextrin [87], which are known to inhibit Aβ aggregation by stabilizing Aβ into non-toxic conformation [86, 88]. In contrast, β-sheet formation by Aβ was largely unaffected by AP (Fig. 11B).

III-2.5 TF potently inhibits polymerization, extension of Aβ42 fiber from fresh Aβ and dissolves preformed fibrils

Several flavonoid molecules inhibit aggregation of Aβ [55, 56]. We examined the activity of the TF or AP to inhibit Aβ42 fibrillogenesis by thioflavin-T binding assay [58, 71]. Freshly dissolved Aβ42 (20 μM) incubated at 37 ºC followed characteristic sigmoidal and revealed nucleation-dependent polymerization model. In the presence of (0-16 μM) TF, final equilibrium of the curve dose dependently decreased (Fig. 12A). Common logarithms of florescence data fitted well in logistic equation (see material and methods) (Fig. 12B). $t/2$ for Aβ42 (20 μM) calculated 23.2, 26.0, 26.9 and 29.2 min, respectively, in presence of 0, 0.5, 1, 2 and 4 μM of TF.

When fresh Aβ42 (20 μM) was incubated with 1.1 μM preformed Aβ42 fibril (seed), the fluorescence increased hyperbolically without lag phase and equilibrium reached much earlier (Fig. 12C). The final equilibrium of the curve decreased dose dependently in presence of TF but the slope of the straight lines remained unchanged (Fig. 12D). A plot between varying concentrations of Aβ42 versus initial rate produced first-order linear equation. This linear equation was also observed in presence of TF (8 μM) with reduced slope (Fig. 12E). The fluorescence of preformed Aβ42 fibrils remained unchanged during incubation but it decreased dose dependently in presence of TF (0-20 μM) (Fig. 12F).

On the other hand, AP (0-40 μM) also decreased the final equilibrium of characteristic sigmoidal curve of Aβ42 (20 μM) and common logarithms of florescence obtained as function of time fitted well in logistic equation (Fig. 13A and B). $t/2$ for Aβ42 was calculated 27.1, 31.0, and 28.3 min, respectively, in presence of 0, 0.5, and 1 μM AP. The final equilibrium of hyperbolic curve of Aβ42 (20 μM) obtained in presence of seed (1.1 μM) decreased dose dependently and the slope of the straight lines remained unchanged (Fig. 13C and D). It also destabilized the preformed Aβ42 fibrils in a dose dependent manner (Fig. 13E). But we could not find the above described pattern of Aβ kinetics at high concentrations of TF or AP; higher

$t/2$ value and decreased slope was observed instead. These suggest that formation of oligomeric complex Aβ at higher molar ratios of these inhibitors can not be ignored. Inhibitory effect of AP on Aβ42 fibrillogenesis was very weak compared to TF. IC_{50} value to inhibit polymerization, extension of Aβ fiber from fresh Aβ and dissolution of preformed Aβ fibrils by 50% is shown in Table 1.

III-2.6 Comparison of inhibition of polymerization and extension kinetics of Aβ

TF potently inhibited kinetics of Aβ aggregation whereas AP was partially effective (Fig. 12 and 13). During Aβ aggregation, monomeric Aβ self-associates forming dimers, trimers and small oligomers [32, 33]. These building block acts as a precursor molecule in which monomers are further added. Both TF and AP decreased the fluorescence during lag and initial fiber elongation phase of Aβ fibrillogenesis (Fig. 14A). AP did not show inhibitory activity at the rapid extension phase of Aβ fibrillogenesis. In contrast, TF was effective even at rapid fiber extension phase, possibly interacting with the oligomers (Fig. 14B and C). TF reduced initial rate of fiber extension of Aβ in a dose dependent manner whereas AP was less efficient (Fig. 14D). These

results indicate that effectiveness of TF over AP is mainly at the fiber extension step. It is possible that TF traps the oligomeric kinetic intermediates of Aβ to limit the fibrillogenesis.

III-2.7 Anti-amyloidogenic and cytoprotective effect of other related biflavonoids

TF showed strong inhibiting effect on Aβ fibrillogenesis and cytotoxicity. To determine whether it is specific to TF or other biflavonoids exert similar effects, we further studied the activities of other biflavonoids (2',8''-biapigenin, amentoflavone and sumaflavone) (Fig. 6) in Aβ mediated toxicity. The cellular assays performed in similar condition showed as low as 2.5 μM of these biflavonoids were enough to protect the cells (~50%) exposed to Aβ (Fig. 15A). Spherical particles, globular oligomers and small oligomers of Aβ42 were also visualized by TEM in presence of each biflavonoid (Fig. 15B). Thioflavin-T binding assay of Aβ42 performed at a concentration used in cell culture (0.5 μM), showed reduction in fluorescence (Fig. 15C). Initial rate of fiber extension of fresh Aβ42 (20 μM) was decreased in presence of each biflavonoid (Fig. 15D). Their activity was in the order of 2',8"-biapigenin > amentoflavone > sumaflavone. Western analysis also showed the

accumulation of Aβ oligomers in presence of each biflavonoids (Fig. 15E). These results demonstrated the similar behaviors of these biflavonoids to inhibit Aβ toxicity.

Accumulation of oligomeric species of Aβ in presence of TF while efficiently rescuing cells exposed to fresh Aβ or enriched Aβ oligomers or fibers suggests that TF possibly binds and neutralizes activity of several species of Aβ formed during aggregation. Whether Aβ oligomers collectively cause neuronal damage or the individual species as observed in crosslinked preparations (Fig. 10A, lane-4) are responsible for the deleterious consequences remain unclear. Earlier work has also shown that oligomers stabilized by the inhibitors are non-toxic [85, 88]. Considerable activity of AP against fresh Aβ42 (Fig. 7A) is comparable to earlier study, which reported the protective effect of AP against Aβ (25-35) [46]. In addition, our result clearly demonstrates AP can not protect the cells exposed to Aβ oligomers, which is more toxic compared to fresh Aβ in the similar condition (Fig. 7A and 10B).

Cellular protection of TF against preformed Aβ fibril suggests that it may also bind to larger polymers or degrade them into non-toxic form (Fig. 10C and 12F). Like several other polyphenols TF and AP destabilized the fibrils [58], we and others did not observe the increment in soluble pool of Aβ

in presence of inhibitors [58, 69]. The experimental evidence shown against the fibril-destabilizing activity of NGDA and curcumin, concluded the inhibition of protofibrils association but not the disintegration of the fibrils [69]. It also suggested some the limitations of the thioflavin-T assay method in this aspect [69, 89], which still remains elusive. Their EM results [69] argued the disappearance of the fibrils in presence of NGDA, curcumin and other polyphenols. The loss or break of highly resistant fibers is unlikely to occur. Preformed fibrils were, indeed, less toxic but AP showed no protective effect (Fig. 10C). This result clearly shows AP may weakly bind oligomers and fibers and hence can not nullify their activity.

It is possible that TF also binds to oligomers or protofibrils as in curcumin [44] and NGDA [69] or alternatively, inhibits their associations. Accumulation of non-toxic Aβ dimers and oligomers in presence of inhibitor as shown here or in other study [85] suggests it might be one of the mechanisms to inactivate Aβ peptide. Our observations on biflavonoids (Fig. 6) are in line with the other studies that indicate dimeric aromatic [90] and small molecules resembling curcumin and congo red structure are better neuroprotective molecule but not simple aromatic or flavonoid molecule despite their anti-amyloidogenic activity [44, 52, 90]. A minimum of two binding sites on the surface of Aβ is suggested to accommodate aromatic groups of the inhibitors

and form hydrogen bond within these pockets [52]. This is likely to be inhibitory mechanism of biflavonoid molecule, which is also proposed for curcumin [52].

In conclusion, several flavonoid molecules may impair the aggregation of the Aβ peptides somehow but most are ineffective to inactivate the toxic species formed during aggregation. Our results demonstrate apigenin itself is not effective against Aβ peptide but it exerts profound activity in its dimeric form as in TF or other biflavonoids. This observation strongly suggests biflavonoid molecules can better satisfy the amyloidogenic cores of Aβ and prevent aggregation as well as cytotoxicity by neutralizing potentially toxic oligomeric precursor molecules of Aβ fibrillogenesis.

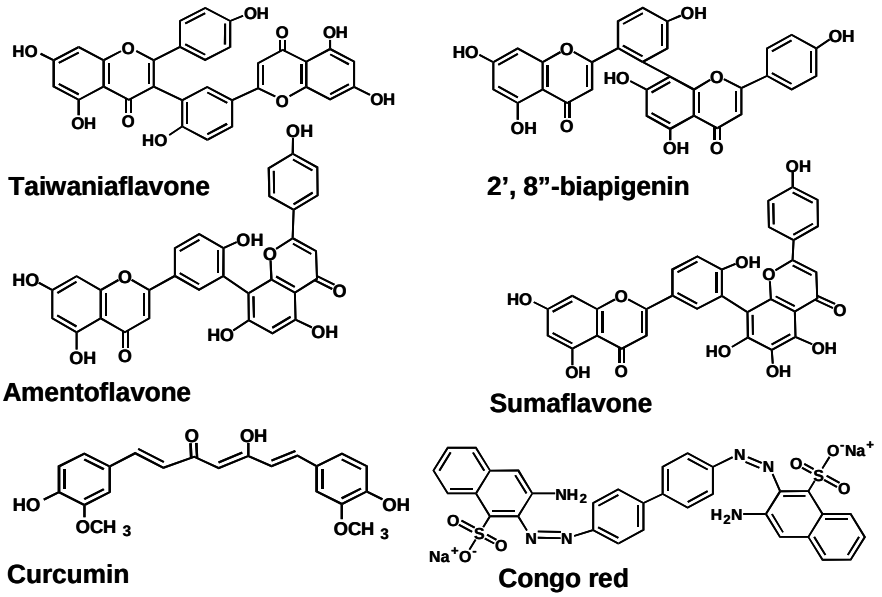

Fig. 6. Chemical structures of biflavonoids and other previously reported anti-amyloidogenic molecules. Structures of taiwaniaflavone and other biflavonoids (2',8"-biapigenin, amentoflavone, and sumaflavone) are shown and compared to curcumin and congo red (structures not drawn to scale).

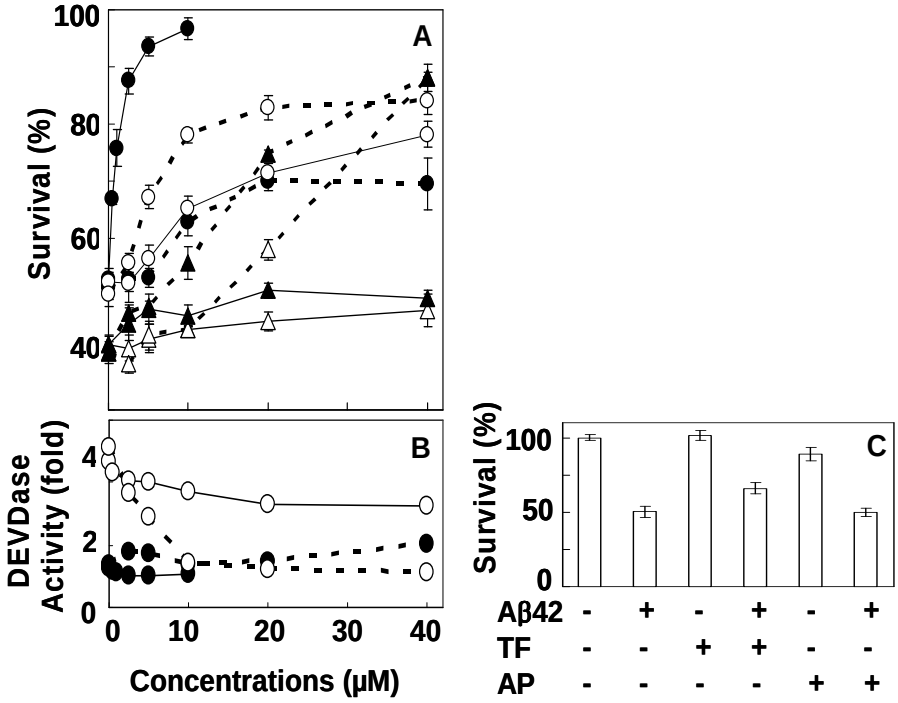

Fig. 7. Effects of taiwaniaflavone (TF) and apigenin (AP) on cellular toxicity of Aβ42 or other toxic insults on cultured SH-SY5Y cells. (A) Cells were treated with 0.5 μM Aβ42 (●), 25 nM STS (○), 1 μM BFA (▲), 1 μM ETO (Δ) in presence of (0-20) μM TF (——) or (0-40) μM AP (----) for 12 h (Aβ42, STS) or 24 h (BFA, ETO). **(B)** Caspase-3/7 like activity of cells incubated with Aβ42 (●) or STS (○) in presence of (0-20 μM) of TF (——) or (0-40) μM AP (----) was monitored after 12 h. **(C)** Cells were pretreated with TF (10 μM) or AP (10 μM). After 12 h, cells were washed and then treated with Aβ42 later. Cell viability **(A, C)** was assessed by MTT reduction assay and survival (%) was compared with untreated cells.

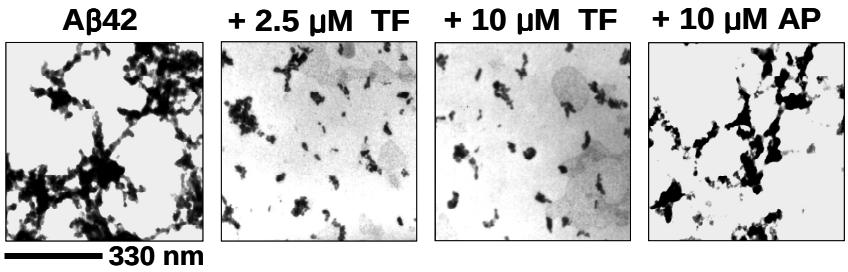

Fig. 8. Effects of TF or AP on Aβ42 morphology. Aβ42 (0.5 μM) either alone or in presence of TF or AP was incubated in PBS at 37 ℃ for 12 h. Aβ42 assemblies formed in the absence or presence of TF or AP was visualized by TEM. Scale bar is shown on the bottom.

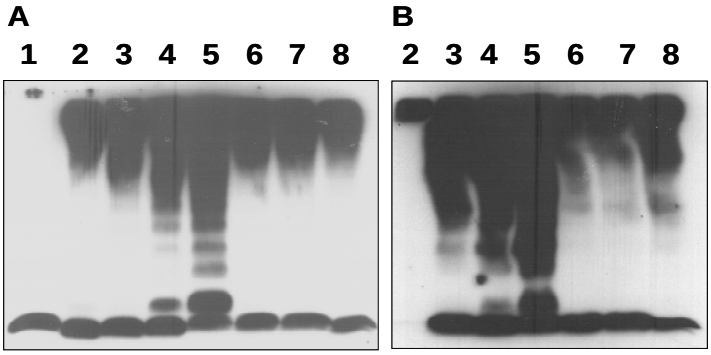

Fig. 9. Biochemical analysis Aβ42 fibrillogenesis. Aβ42 (0.5 μM) either alone or in presence TF or AP was incubated for 3 h **(A)** or 12 h **(B)**. The reaction mixtures were crosslinked by glutaraldehyde (0.01%) except for freshly dissolved Aβ42 (control), which was boiled for 5 min before gel running. A 20 μl sample from each reaction mixture was loaded on 16% SDS-PAGE, transferred to PVDF membrane, and probed with monoclonal antibody to Aβ (6E10). Lane-1, Aβ42 (control); 2, Aβ42 aggregated [3 h **(A)** and 12h **(B)**]; 3-5, Aβ42 in presence of TF (2.5, 5 and 10) μM [3 h **(A)** and 12 h **(B)**]; 6-8, Aβ42 in presence of AP (2.5, 5 and 10) μM [3 h **(A)** and 12 h **(B)**]. A typical experiment is shown.

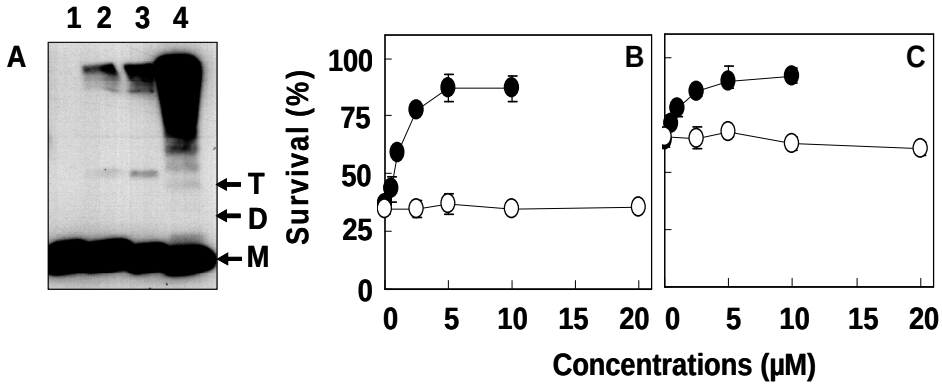

Fig. 10. TF rescues cells exposed to Aβ42 oligomers and fibers. Aβ42 oligomers and fibers were isolated as described in material and methods. **(A)** A 10 µl freshly prepared oligomers with or without crosslinking were separated on 16% SDS-PAGE, transferred to PVDF membrane and probed with monoclonal antibody 6E10. Lane-1, Aβ42 (control/boiled); 2, Aβ42 from the reaction mixture subjected to oligomerization; 3, Aβ42 oligomers (supernatant) after centrifugation; 4, crosslinked oligomers. Cells were treated with Aβ42 (0.5 µM) oligomers **(B)** or fibers (0.5 µM) **(C)** in presence (0-10) µM of TF (●) or (0-20) µM AP (○) for 12 h. Cell viability was assessed by MTT reduction assay and cell survival (%) was compared with untreated cells. A typical experiment is shown and data indicate mean ± S.D of triplicate samples.

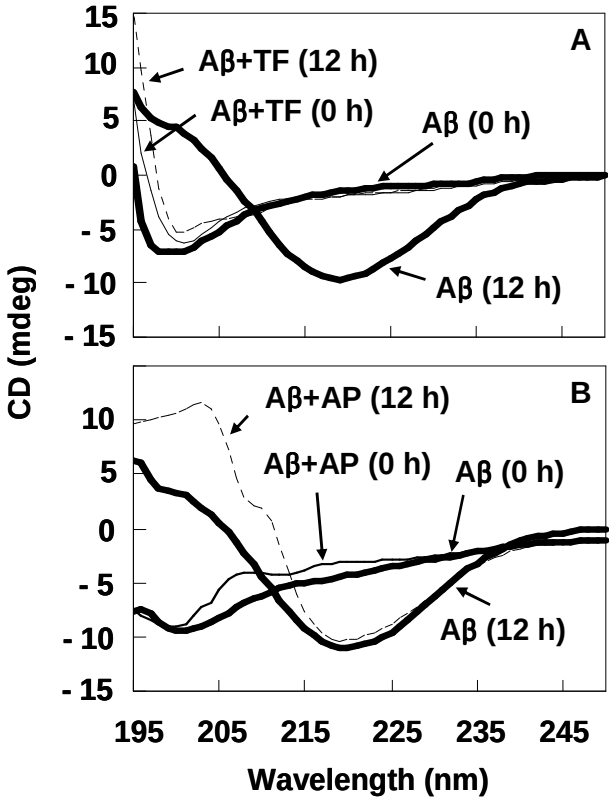

Fig.11. TF inhibits structural transformation of Aβ42. Aβ42 (20 μM) alone or in presence of **(A)** TF (20 μM) or **(B)** AP (20 μM) was incubated in PBS at 37 °C for 0 or 12 h as indicated. Spectra were obtained by subtracting buffer background as described in materials and methods.

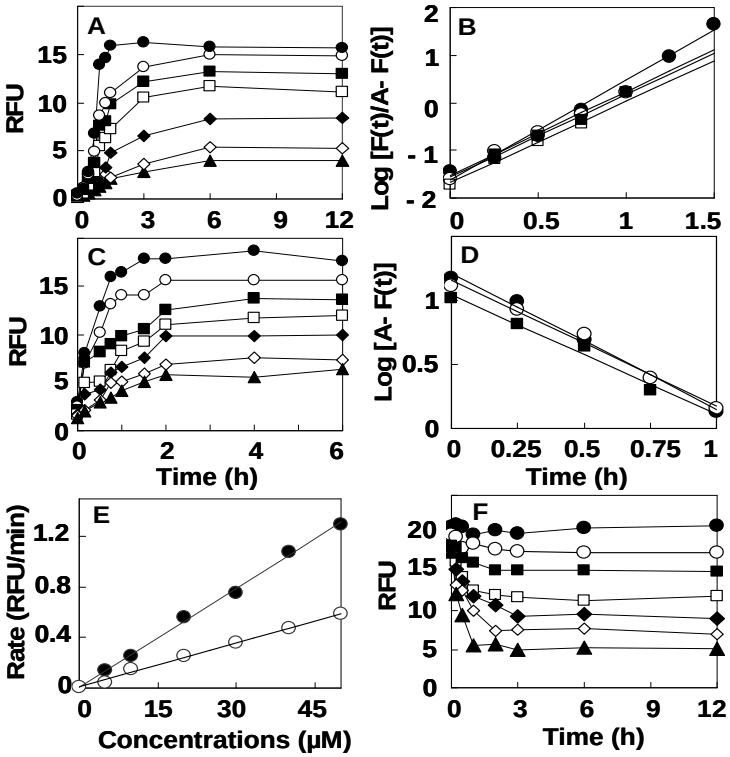

Fig. 12. TF potently inhibits of Aβ42 fibrillogenesis. **(A)** Inhibition of Aβ42 polymerization. Aβ42 (20 μM) was incubated in PBS at 37 °C in presence of 0 (●), 0.5 (○), 1 (■), 2 (□), 4 (◆) 8 (◊), 16 (▲) μM TF for 0-12 h. **(B)** Logarithmic plot of $F(t)/A-F(t)$ versus reaction time obtained from polymerization assay. **(C)** Inhibition of Aβ42 fiber extension from fresh Aβ42. **(D)** Logarithmic plot of $A-F(t)$ versus reaction time obtained from fiber extension assay. **(E)** Effect of Aβ42 concentrations on the initial rate of Aβ42 fibril extension with (○) or without (●) TF (8 μM). **(F)** Dissolution of preformed Aβ42 fibrils in presence of 0 (●), 1 (○), 2 (■), 4 (□), 8 (◆) 16 (◊), 20 (▲) μM TF.

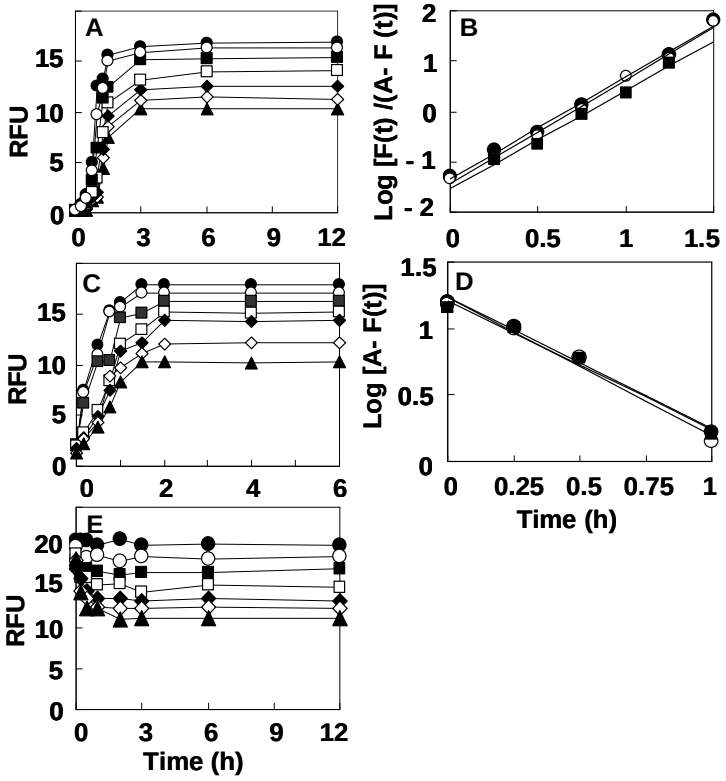

Fig. 13. AP partially inhibits of Aβ42 fibrillogenesis. (A) Inhibition of Aβ42 polymerization. Aβ42 (20 μM) was incubated in PBS at 37 °C in presence of 0 (●), 1.25 (○), 2.5 (■), 5 (□), 10 (◆), 20 (◊), 40 (▲) μM AP for 0-12 h. **(B)** Logarithmic plot of $F(t)/A-F(t)$ versus reaction time obtained from polymerization assay where A indicates $F(\infty)$. **(C)** Inhibition of Aβ42 fiber extension of fresh Aβ42 in presence of 0 (●), 1.25 (○), 2.5 (■), 5 (□), 10 (◆), 20 (◊), 40 (▲) μM AP. **(D)** Logarithmic plot of $A-F(t)$ versus reaction time obtained from extension assay. **(E)** Dissolution of preformed Aβ42 fibrils in presence of 0 (●), 1.25 (○), 2.5 (■), 5 (□), 10 (◆), 20 (◊), 40 (▲) μM AP.

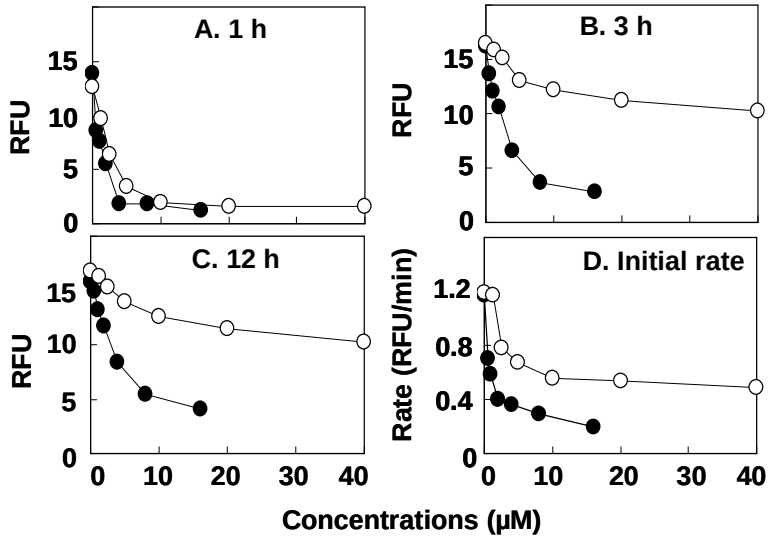

Fig. 14. Kinetic analysis of polymerization and extension kinetics Aβ42. **(A-C)** fresh Aβ42 (20 μM) was incubated in PBS at 37 °C in presence of varying concentrations of TF (●) or AP (○) for 0, 3, and 12 h. A plot of RFU versus concentrations at indicated time point is shown. **(D)** Effect of TF or AP concentrations on initial rate of fibril extension of Aβ42. Preformed Aβ42 fibril (1.1 μM) was added to fresh Aβ42 (20 μM) and incubated in PBS at 37 °C for 0-12 h in presence varying concentrations of TF (●) or AP. A plot of initial rate versus varying concentrations of TF or AP is shown.

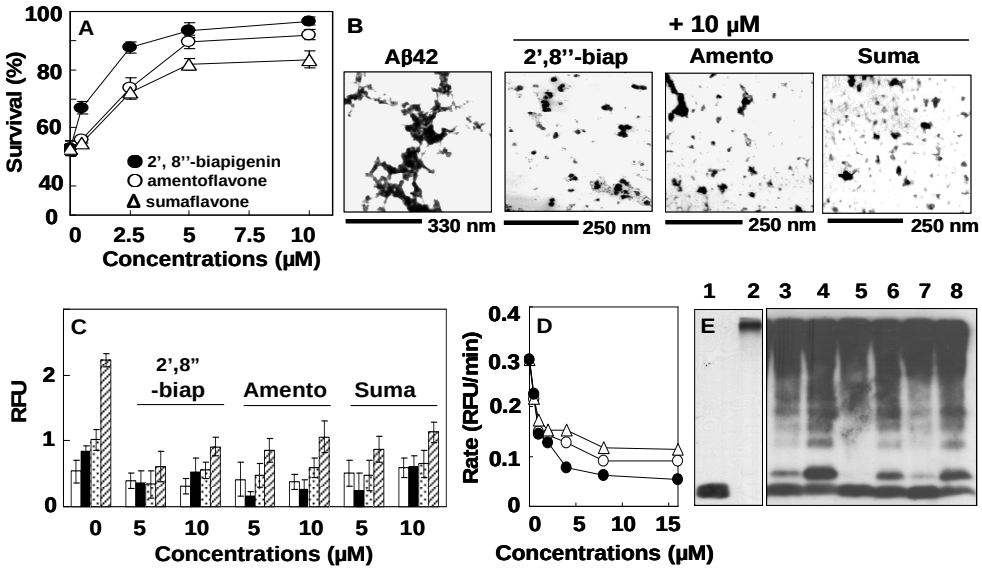

Fig. 15. Effects of other related biflavonoids on Aβ42 induced cellular toxicity and fibrillogenesis. (A) Cells were treated with Aβ (0.5 μM) in presence of indicated biflavonoids for 12 h. Cell viability was assessed as described in material and method. **(B)** Aβ assemblies formed either alone or in presence of indicated biflavonoids were visualized by TEM **(C)** Thioflavin-T assay of Aβ42 (0.5 μM) in presence of indicated biflavonoids. RFU measured at 0 h (white bar), 3 h (black bar), 6 h (dotted bar) and 12 h (hatched bar) is shown. **(D)** A plot of initial rate of fresh Aβ42 (20 μM) fiber extension with seed is shown in presence of (0-16) μM of 2',8"-biap (●) or amento (○) or suma (Δ). **(E)** Western blot analysis of Aβ42 (0.5 μM) fibrillogenesis. Lane-1, Aβ42 (control/boiled); 2, Aβ42 aggregated (12 h); 3-4, Aβ42 in presence of (●), 5 and 10 μM; 5-6, (○) 5 and 10 μM; 7-8, (Δ) 5 and 10 μM.

Table 1. IC_{50} TF or other biflavonoids and apigenin.

Chemicals	Polymerization (μM)	Extension (μM)	Destabilization (μM)
TF	2.5	3.1	5.0
AP	25	40	> 40
2',8''-biapi	3.1	3.5	6.3
Amento	3.5	6.3	5.0
Suma	6.3	7.9	5.6

IC_{50} is defined as the concentrations of TF or other biflavonoids or AP required to inhibit polymerization, fiber extension of fresh Aβ42 and destabilization of preformed Aβ42 fibrils to 50% of control value. The average fluorescence without compounds in the corresponding assays was regarded as 100%. Fluorescence (%) versus concentrations of compounds in log (μM) yielded a sigmoidal curve and IC_{50} was determined accordingly [58].

III-3. Higher expression and stability Aβ42 as fusion to D-ribose periplasmic protein (RbsB)

III-3.1 Higher expression of Rbsb-Aβ42 fusion protein

Aβ42 is a difficult-to-express peptide [79]. RbsB protein [78] was highly overexpressed and thermostable too. This fusion protein construct (Fig. 16A) enhanced the overexpression of Aβ42. Possibly, because of higher expression of RbsB-Aβ42 fusion protein, it accumulated in the insoluble fraction. RbsB could not enhance the solubility of Aβ42 but it appeared as useful fusion tag to augment the yield of target (Fig. 16B). Whether RbsB can offer solubility to less complex target than Aβ42 remains to be studied.

III-3.2 Solubilization of RbsB-Aβ42

Because almost all of the fusion protein was recovered in insoluble fraction, it required simple purification process. Inclusion bodies were solubilized (Fig. 16C) in urea buffer (materials and method). Fusion protein was clarified by centrifugation and dialyzed against renaturation buffers. The yield of the intact fusion protein was estimated to be >100 mg per liter

bacterial culture, which is quite high compared to previous report [74]. Laborious and expensive method of chromatographic protein purification processes were skipped as it was found to be pure enough. The fusion protein was stored at 4 °C.

III-3.3 Application of RbsB fusion protein

Highly overexpressed target proteins or peptides usually results into insoluble aggregates and *in vitro* renaturation of the solubilized inclusion bodies remains uncertain [22]. Efficient refolding of the test peptide (Fig. 16C) indicated that RbsB fusion protein provides proper folding of the targets fused to them. Prevention of aggregation of the fused Aβ42 stored 4 °C over a month, further suggested that the higher expression of this export protein (RbsB) accompanied by thermostablity (Fig. 1B) and foldase activity [78] may have been involved to improve the expression and stability of Aβ42.

In summary, RbsB offers some advantages over various fusion partners due to its higher level of expression and stability of aggregation prone peptide. Easier solubilization and efficient renaturation processes without chromatographic purifications are important aspect of this fusion partner. It also provides easier handling and storage of the targets and hence

can be considered as convenient tool. Finally, this expression system appears easier and inexpensive method to produce antigenic sequences of the heterologous proteins and peptides to generate antibodies.

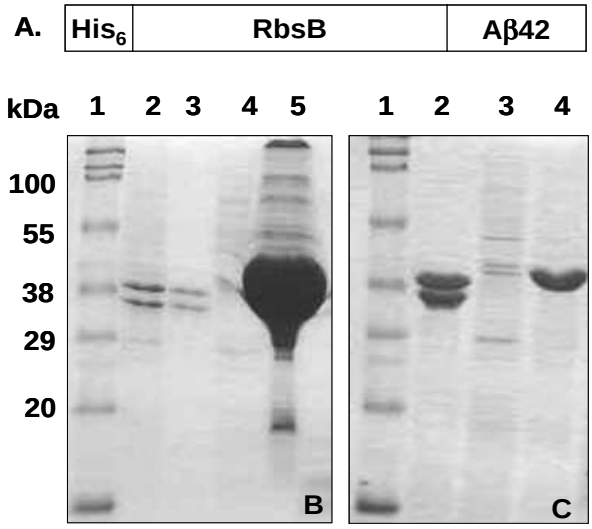

Fig. 16. Construction of RbsB fusion protein consisting vector and overexpression of Aβ42. (A) Schematic representation of the RbsB fusion constructs used to overexpress Aβ42. **(B)** SDS-PAGE analysis of Aβ42 overexpression as fusion to RbsB. Lane-1, protein marker; 2, RbsB protein (before boiling); 3, RbsB protein after boiling 10 min boiling; 4, soluble fraction of Aβ42 fused protein; and 5, insoluble fraction of the Aβ42 fused protein. Ten times more proteins were loaded in lane 5 than in others. **(C)** Solubilization of the fusion protein. Lane-1, protein marker; 2, RbsB protein (control); 3, cell extract of the Aβ42 fused protein; 4, urea solubilized Aβ42 fused protein. Equal amount of protein was loaded in each lane. Expected molecular weights are indicated on the left side of each gel.

IV-4. Further study

IV-4.1 Inhibition of Aβ aggregation by β-sheet breaker peptide

Short synthetic peptides capable of binding Aβ but unable to become part of β-sheet structure are also increasingly appreciated to inhibit Aβ aggregation [47]. These β-sheet breaker peptides are shown to reduce amyloid load in transgenic Alzheimer's models. The pentapeptide (GVVIA) designed using C-terminal sequence of Aβ is reported to inhibit Aβ fibrillogenesis and cytotoxicity [91]. Hydrophobic interaction of side chains of Ile of inhibitor (GVVIA) and Val (39 residue) of template Aβ42 is shown to stabilize the complex [91]. In this study, GVVIA inhibitor sequence is coupled to Aβ42 following a flexible linker residue (Gly). Aβ42-inhibitor complex is subcloned after a fusion protein (GroES), which assist overexpression of Aβ42 in insoluble form. This Aβ42-inhibitor complex protein is expected to be soluble and non-toxic.

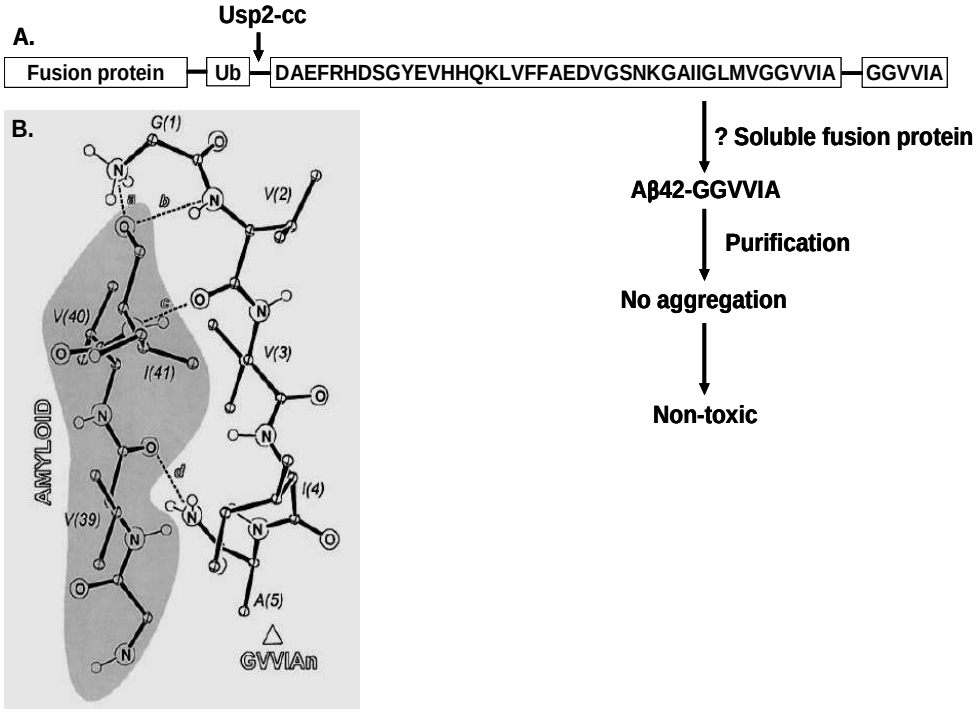

Fig. 17. Construction of recombinant Aβ42-GGVVIA. (A) Schematic representation of the construct (not drawn to scale) and anticipated flow chart to neutralize the effects of Aβ42. **(B)** Possible interaction of the pentapeptide inhibitor (GVVIA) and C-terminus amyloidogenic sequences of Aβ42 is shown [91]. Letters a, b, c and denotes expected hydrogen bonds and symbol (arrow head) shows direction of β-sheet in **(B).**

V. REFERENCES

[1] J. Hardy, and D. Allsop, Amyloid deposition as the central event in the aetiology of Alzheimer's disease, Trends Pharmacol Sci 12 (1991) 383-388.

[2] A. Goate, M. C. Chartier-Harlin, M. Mullan, J. Brown, F. Crawford, L. Fidani, L. Giuffra, A. Haynes, N. Irving, L. James, and et al., Segregation of a missense mutation in the amyloid precursor protein gene with familial Alzheimer's disease, Nature 349 (1991) 704-706.

[3] Y. H. Suh, An etiological role of amyloidogenic carboxyl-terminal fragments of the beta-amyloid precursor protein in Alzheimer's disease, J Neurochem 68 (1997) 1781-1791.

[4] Y. H. Suh, and F. Checler, Amyloid precursor protein, presenilins, and alpha-synuclein: molecular pathogenesis and pharmacological applications in Alzheimer's disease, Pharmacol Rev 54 (2002) 469-525.

[5] D. J. Selkoe, Alzheimer's disease: genes, proteins, and therapy, Physiol Rev 81 (2001) 741-766.

[6] L. Lannfelt, Genetics of Alzheimer's disease, Acta Neurol Scand Suppl 168 (1996) 25-27.

[7] W. G. Annaert, L. Levesque, K. Craessaerts, I. Dierinck, G. Snellings, D. Westaway, P. S. George-Hyslop, B. Cordell, P. Fraser, and B. De Strooper, Presenilin 1 controls gamma-secretase processing of amyloid precursor protein in pre-golgi compartments of hippocampal neurons, J Cell Biol 147 (1999) 277-294.

[8] F. S. Esch, P. S. Keim, E. C. Beattie, R. W. Blacher, A. R. Culwell, T. Oltersdorf, D. McClure, and P. J. Ward, Cleavage of amyloid beta peptide during constitutive processing of its precursor, Science 248 (1990) 1122-1124.

[9] J. T. Jarrett, E. P. Berger, and P. T. Lansbury, Jr., The carboxy terminus of the beta amyloid protein is critical for the seeding of amyloid formation: implications for the pathogenesis of Alzheimer's disease, Biochemistry 32 (1993) 4693-4697.

[10] R. Kayed, E. Head, J. L. Thompson, T. M. McIntire, S. C. Milton, C. W. Cotman, and C. G. Glabe, Common structure of soluble amyloid oligomers implies common mechanism of pathogenesis, Science 300 (2003) 486-489.

[11] W. Kim, Y. Kim, J. Min, D. J. Kim, Y. T. Chang, and M. H. Hecht, A high-throughput screen for compounds that inhibit aggregation of the Alzheimer's peptide, ACS Chem Biol 1 (2006) 461-469.

[12] D. M. Walsh, and D. J. Selkoe, A beta oligomers - a decade of discovery, J Neurochem 101 (2007) 1172-1184.

[13] T. Tomita, K. Maruyama, T. C. Saido, H. Kume, K. Shinozaki, S. Tokuhiro, A. Capell, J. Walter, J. Grunberg, C. Haass, T. Iwatsubo, and K. Obata, The presenilin 2 mutation (N141I) linked to familial Alzheimer disease (Volga German families) increases the secretion of amyloid beta protein ending at the 42nd (or 43rd) residue, Proc Natl Acad Sci U S A 94 (1997) 2025-2030.

[14] D. J. Selkoe, and M. B. Podlisny, Deciphering the genetic basis of Alzheimer's disease, Annu Rev Genomics Hum Genet 3 (2002) 67-99.

[15] G. G. Glenner, and C. W. Wong, Alzheimer's disease and Down's syndrome: sharing of a unique cerebrovascular amyloid fibril protein, Biochem Biophys Res Commun 122 (1984) 1131-1135.

[16] G. Hannig, and S. C. Makrides, Strategies for optimizing heterologous protein expression in Escherichia coli, Trends Biotechnol 16 (1998) 54-60.

[17] H. P. Sorensen, and K. K. Mortensen, Soluble expression of recombinant proteins in the cytoplasm of Escherichia coli, Microb Cell Fact 4 (2005) 1.

[18] A. M. Catanzariti, T. A. Soboleva, D. A. Jans, P. G. Board, and R. T.

Baker, An efficient system for high-level expression and easy purification of authentic recombinant proteins, Protein Sci 13 (2004) 1331-1339.

[19] P. A. Nygren, S. Stahl, and M. Uhlen, Engineering proteins to facilitate bioprocessing, Trends Biotechnol 12 (1994) 184-188.

[20] H. P. Sorensen, H. U. Sperling-Petersen, and K. K. Mortensen, Production of recombinant thermostable proteins expressed in Escherichia coli: completion of protein synthesis is the bottleneck, J Chromatogr B Analyt Technol Biomed Life Sci 786 (2003) 207-214.

[21] F. U. Hartl, and M. Hayer-Hartl, Molecular chaperones in the cytosol: from nascent chain to folded protein, Science 295 (2002) 1852-1858.

[22] J. G. Thomas, A. Ayling, and F. Baneyx, Molecular chaperones, folding catalysts, and the recovery of active recombinant proteins from E. coli. To fold or to refold, Appl Biochem Biotechnol 66 (1997) 197-238.

[23] R. B. Kapust, and D. S. Waugh, Escherichia coli maltose-binding protein is uncommonly effective at promoting the solubility of polypeptides to which it is fused, Protein Sci 8 (1999) 1668-1674.

[24] E. R. LaVallie, E. A. DiBlasio-Smith, L. A. Collins-Racie, Z. Lu, and J. M. McCoy, Thioredoxin and related proteins as multifunctional fusion

tags for soluble expression in E. coli, Methods Mol Biol 205 (2003) 119-140.

[25] V. De Marco, G. Stier, S. Blandin, and A. de Marco, The solubility and stability of recombinant proteins are increased by their fusion to NusA, Biochem Biophys Res Commun 322 (2004) 766-771.

[26] G. S. Waldo, B. M. Standish, J. Berendzen, and T. C. Terwilliger, Rapid protein-folding assay using green fluorescent protein, Nat Biotechnol 17 (1999) 691-695.

[27] L. A. Collins-Racie, J. M. McColgan, K. L. Grant, E. A. DiBlasio-Smith, J. M. McCoy, and E. R. LaVallie, Production of recombinant bovine enterokinase catalytic subunit in Escherichia coli using the novel secretory fusion partner DsbA, Biotechnology (N Y) 13 (1995) 982-987.

[28] C. F. Zheng, T. Simcox, L. Xu, and P. Vaillancourt, A new expression vector for high level protein production, one step purification and direct isotopic labeling of calmodulin-binding peptide fusion proteins, Gene 186 (1997) 55-60.

[29] Y. Nomine, T. Ristriani, C. Laurent, J. F. Lefevre, E. Weiss, and G. Trave, Formation of soluble inclusion bodies by hpv e6 oncoprotein fused to maltose-binding protein, Protein Expr Purif 23 (2001) 22-32.

[30] J. D. Fox, R. B. Kapust, and D. S. Waugh, Single amino acid substitutions on the surface of Escherichia coli maltose-binding protein can have a profound impact on the solubility of fusion proteins, Protein Sci 10 (2001) 622-630.

[31] A. de Marco, E. Casatta, S. Savaresi, and A. Geerlof, Recombinant proteins fused to thermostable partners can be purified by heat incubation, J Biotechnol 107 (2004) 125-133.

[32] D. M. Walsh, D. M. Hartley, Y. Kusumoto, Y. Fezoui, M. M. Condron, A. Lomakin, G. B. Benedek, D. J. Selkoe, and D. B. Teplow, Amyloid beta-protein fibrillogenesis. Structure and biological activity of protofibrillar intermediates, J Biol Chem 274 (1999) 25945-25952.

[33] B. A. Chromy, R. J. Nowak, M. P. Lambert, K. L. Viola, L. Chang, P. T. Velasco, B. W. Jones, S. J. Fernandez, P. N. Lacor, P. Horowitz, C. E. Finch, G. A. Krafft, and W. L. Klein, Self-assembly of Abeta(1-42) into globular neurotoxins, Biochemistry 42 (2003) 12749-12760.

[34] T. Kawarabayashi, M. Shoji, L. H. Younkin, L. Wen-Lang, D. W. Dickson, T. Murakami, E. Matsubara, K. Abe, K. H. Ashe, and S. G. Younkin, Dimeric amyloid beta protein rapidly accumulates in lipid rafts followed by apolipoprotein E and phosphorylated tau accumulation in the Tg2576 mouse model of Alzheimer's disease, J

Neurosci 24 (2004) 3801-3809.

[35] J. Hardy, and D. J. Selkoe, The amyloid hypothesis of Alzheimer's disease: progress and problems on the road to therapeutics, Science 297 (2002) 353-356.

[36] E. Head, E. G. Barrett, M. P. Murphy, P. Das, M. Nistor, F. Sarsoza, C. C. Glabe, R. Kayed, S. Milton, V. Vasilevko, N. W. Milgram, M. G. Agadjanyan, D. H. Cribbs, and C. W. Cotman, Immunization with fibrillar Abeta(1-42) in young and aged canines: Antibody generation and characteristics, and effects on CSF and brain Abeta, Vaccine 24 (2006) 2824-2834.

[37] R. Kayed, and C. G. Glabe, Conformation-dependent anti-amyloid oligomer antibodies, Methods Enzymol 413 (2006) 326-344.

[38] O. Berezovska, C. Jack, P. McLean, J. C. Aster, C. Hicks, W. Xia, M. S. Wolfe, W. T. Kimberly, G. Weinmaster, D. J. Selkoe, and B. T. Hyman, Aspartate mutations in presenilin and gamma-secretase inhibitors both impair notch1 proteolysis and nuclear translocation with relative preservation of notch1 signaling, J Neurochem 75 (2000) 583-593.

[39] A. Petit, F. Bihel, C. Alves da Costa, O. Pourquie, F. Checler, and J. L. Kraus, New protease inhibitors prevent gamma-secretase-mediated

production of Abeta40/42 without affecting Notch cleavage, Nat Cell Biol 3 (2001) 507-511.

[40] D. Commenges, V. Scotet, S. Renaud, H. Jacqmin-Gadda, P. Barberger-Gateau, and J. F. Dartigues, Intake of flavonoids and risk of dementia, Eur J Epidemiol 16 (2000) 357-363.

[41] L. Puglielli, R. E. Tanzi, and D. M. Kovacs, Alzheimer's disease: the cholesterol connection, Nat Neurosci 6 (2003) 345-351.

[42] T. D. Rea, J. C. Breitner, B. M. Psaty, A. L. Fitzpatrick, O. L. Lopez, A. B. Newman, W. R. Hazzard, P. P. Zandi, G. L. Burke, C. G. Lyketsos, C. Bernick, and L. H. Kuller, Statin use and the risk of incident dementia: the Cardiovascular Health Study, Arch Neurol 62 (2005) 1047-1051.

[43] M. Necula, R. Kayed, S. Milton, and C. G. Glabe, Small molecule inhibitors of aggregation indicate that amyloid beta oligomerization and fibrillization pathways are independent and distinct, J Biol Chem 282 (2007) 10311-10324.

[44] F. Yang, G. P. Lim, A. N. Begum, O. J. Ubeda, M. R. Simmons, S. S. Ambegaokar, P. P. Chen, R. Kayed, C. G. Glabe, S. A. Frautschy, and G. M. Cole, Curcumin inhibits formation of amyloid beta oligomers and fibrils, binds plaques, and reduces amyloid in vivo, J Biol Chem 280

(2005) 5892-5901.

[45] Y. S. Han, W. H. Zheng, S. Bastianetto, J. G. Chabot, and R. Quirion, Neuroprotective effects of resveratrol against beta-amyloid-induced neurotoxicity in rat hippocampal neurons: involvement of protein kinase C, Br J Pharmacol 141 (2004) 997-1005.

[46] Y. T. Choi, C. H. Jung, S. R. Lee, J. H. Bae, W. K. Baek, M. H. Suh, J. Park, C. W. Park, and S. I. Suh, The green tea polyphenol (-)-epigallocatechin gallate attenuates beta-amyloid-induced neurotoxicity in cultured hippocampal neurons, Life Sci 70 (2001) 603-614.

[47] Y. Nakagami, S. Nishimura, T. Murasugi, I. Kaneko, M. Meguro, S. Marumoto, H. Kogen, K. Koyama, and T. Oda, A novel beta-sheet breaker, RS-0406, reverses amyloid beta-induced cytotoxicity and impairment of long-term potentiation in vitro, Br J Pharmacol 137 (2002) 676-682.

[48] A. Lorenzo, and B. A. Yankner, Beta-amyloid neurotoxicity requires fibril formation and is inhibited by congo red, Proc Natl Acad Sci U S A 91 (1994) 12243-12247.

[49] Y. Porat, A. Abramowitz, and E. Gazit, Inhibition of amyloid fibril formation by polyphenols: structural similarity and aromatic interactions as a common inhibition mechanism, Chem Biol Drug Des

67 (2006) 27-37.

[50] F. G. De Felice, M. N. Vieira, L. M. Saraiva, J. D. Figueroa-Villar, J. Garcia-Abreu, R. Liu, L. Chang, W. L. Klein, and S. T. Ferreira, Targeting the neurotoxic species in Alzheimer's disease: inhibitors of Abeta oligomerization, Faseb J 18 (2004) 1366-1372.

[51] K. H. Lee, B. H. Shin, K. J. Shin, D. J. Kim, and J. Yu, A hybrid molecule that prohibits amyloid fibrils and alleviates neuronal toxicity induced by beta-amyloid (1-42), Biochem Biophys Res Commun 328 (2005) 816-823.

[52] A. A. Reinke, and J. E. Gestwicki, Structure-activity relationships of amyloid beta-aggregation inhibitors based on curcumin: influence of linker length and flexibility, Chem Biol Drug Des 70 (2007) 206-215.

[53] Y. Luo, J. V. Smith, V. Paramasivam, A. Burdick, K. J. Curry, J. P. Buford, I. Khan, W. J. Netzer, H. Xu, and P. Butko, Inhibition of amyloid-beta aggregation and caspase-3 activation by the Ginkgo biloba extract EGb761, Proc Natl Acad Sci U S A 99 (2002) 12197-12202.

[54] Z. Yao, K. Drieu, and V. Papadopoulos, The Ginkgo biloba extract EGb 761 rescues the PC12 neuronal cells from beta-amyloid-induced cell death by inhibiting the formation of beta-amyloid-derived diffusible

neurotoxic ligands, Brain Res 889 (2001) 181-190.

[55] K. Ono, T. Hamaguchi, H. Naiki, and M. Yamada, Anti-amyloidogenic effects of antioxidants: implications for the prevention and therapeutics of Alzheimer's disease, Biochim Biophys Acta 1762 (2006) 575-586.

[56] C. Ramassamy, Emerging role of polyphenolic compounds in the treatment of neurodegenerative diseases: a review of their intracellular targets, Eur J Pharmacol 545 (2006) 51-64.

[57] C. N. Wang, C. W. Chi, Y. L. Lin, C. F. Chen, and Y. J. Shiao, The neuroprotective effects of phytoestrogens on amyloid beta protein-induced toxicity are mediated by abrogating the activation of caspase cascade in rat cortical neurons, J Biol Chem 276 (2001) 5287-5295.

[58] K. Ono, Y. Yoshiike, A. Takashima, K. Hasegawa, H. Naiki, and M. Yamada, Potent anti-amyloidogenic and fibril-destabilizing effects of polyphenols in vitro: implications for the prevention and therapeutics of Alzheimer's disease, J Neurochem 87 (2003) 172-181.

[59] Y. R. Pokharel, J. W. Yang, J. Y. Kim, H. W. Oh, H. G. Jeong, E. R. Woo, and K. W. Kang, Potent inhibition of the inductions of inducible nitric oxide synthase and cyclooxygenase-2 by taiwaniaflavone, Nitric Oxide 15 (2006) 217-225.

[60] C. Su, F. Wang, D. Ciolek, and Y. C. Pan, Electrophoresis of proteins and protein-protein complexes in native polyacrylamide gels using a horizontal gel apparatus, Anal Biochem 223 (1994) 93-98.

[61] A. Evangelou, C. Zikos, E. Livaniou, and G. P. Evangelatos, High-yield, solid-phase synthesis of humanin, an Alzheimer's disease associated, novel 24-mer peptide which contains a difficult sequence, J Pept Sci 10 (2004) 631-635.

[62] B. C. Baliga, P. A. Colussi, S. H. Read, M. M. Dias, D. A. Jans, and S. Kumar, Role of prodomain in importin-mediated nuclear localization and activation of caspase-2, J Biol Chem 278 (2003) 4899-4905.

[63] W. L. Klein, Abeta toxicity in Alzheimer's disease: globular oligomers (ADDLs) as new vaccine and drug targets, Neurochem Int 41 (2002) 345-352.

[64] M. D. Kirkitadze, M. M. Condron, and D. B. Teplow, Identification and characterization of key kinetic intermediates in amyloid beta-protein fibrillogenesis, J Mol Biol 312 (2001) 1103-1119.

[65] D. H. Shin, Y. C. Bae, J. S. Kim-Han, J. H. Lee, I. Y. Choi, K. H. Son, S. S. Kang, W. K. Kim, and B. H. Han, Polyphenol amentoflavone affords neuroprotection against neonatal hypoxic-ischemic brain damage via multiple mechanisms, J Neurochem 96 (2006) 561-572.

[66] Y. Liu, D. A. Peterson, H. Kimura, and D. Schubert, Mechanism of cellular 3-(4,5-dimethylthiazol-2-yl)-2,5-diphenyltetrazolium bromide (MTT) reduction, J Neurochem 69 (1997) 581-593.

[67] D. M. Walsh, A. Lomakin, G. B. Benedek, M. M. Condron, and D. B. Teplow, Amyloid beta-protein fibrillogenesis. Detection of a protofibrillar intermediate, J Biol Chem 272 (1997) 22364-22372.

[68] M. R. Nichols, M. A. Moss, D. K. Reed, S. Cratic-McDaniel, J. H. Hoh, and T. L. Rosenberry, Amyloid-beta protofibrils differ from amyloid-beta aggregates induced in dilute hexafluoroisopropanol in stability and morphology, J Biol Chem 280 (2005) 2471-2480.

[69] M. A. Moss, N. H. Varvel, M. R. Nichols, D. K. Reed, and T. L. Rosenberry, Nordihydroguaiaretic acid does not disaggregate beta-amyloid(1-40) protofibrils but does inhibit growth arising from direct protofibril association, Mol Pharmacol 66 (2004) 592-600.

[70] K. Zou, J. S. Gong, K. Yanagisawa, and M. Michikawa, A novel function of monomeric amyloid beta-protein serving as an antioxidant molecule against metal-induced oxidative damage, J Neurosci 22 (2002) 4833-4841.

[71] H. Naiki, and K. Nakakuki, First-order kinetic model of Alzheimer's beta-amyloid fibril extension in vitro, Lab Invest 74 (1996) 374-383.

[72] H. Naiki, K. Hasegawa, I. Yamaguchi, H. Nakamura, F. Gejyo, and K. Nakakuki, Apolipoprotein E and antioxidants have different mechanisms of inhibiting Alzheimer's beta-amyloid fibril formation in vitro, Biochemistry 37 (1998) 17882-17889.

[73] D. N. Collier, S. M. Strobel, and P. J. Bassford, Jr., SecB-independent export of Escherichia coli ribose-binding protein (RBP): some comparisons with export of maltose-binding protein (MBP) and studies with RBP-MBP hybrid proteins, J Bacteriol 172 (1990) 6875-6884.

[74] E. K. Lee, J. H. Hwang, D. Y. Shin, D. I. Kim, and Y. J. Yoo, Production of recombinant amyloid-beta peptide 42 as an ubiquitin extension, Protein Expr Purif 40 (2005) 183-189.

[75] M. P. Malakhov, M. R. Mattern, O. A. Malakhova, M. Drinker, S. D. Weeks, and T. R. Butt, SUMO fusions and SUMO-specific protease for efficient expression and purification of proteins, J Struct Funct Genomics 5 (2004) 75-86.

[76] P. Genevaux, F. Keppel, F. Schwager, P. S. Langendijk-Genevaux, F. U. Hartl, and C. Georgopoulos, In vivo analysis of the overlapping functions of DnaK and trigger factor, EMBO Rep 5 (2004) 195-200.

[77] T. Maier, L. Ferbitz, E. Deuerling, and N. Ban, A cradle for new proteins: trigger factor at the ribosome, Curr Opin Struct Biol 15

(2005) 204-212.

[78] A. Ideno, M. Furutani, T. Iwabuchi, T. Iida, Y. Iba, Y. Kurosawa, H. Sakuraba, T. Ohshima, Y. Kawarabayashi, and T. Maruyama, Expression of foreign proteins in Escherichia coli by fusing with an archaeal FK506 binding protein, Appl Microbiol Biotechnol 64 (2004) 99-105.

[79] C. Wurth, N. K. Guimard, and M. H. Hecht, Mutations that reduce aggregation of the Alzheimer's Abeta42 peptide: an unbiased search for the sequence determinants of Abeta amyloidogenesis, J Mol Biol 319 (2002) 1279-1290.

[80] H. Dobeli, N. Draeger, G. Huber, P. Jakob, D. Schmidt, B. Seilheimer, D. Stuber, B. Wipf, and M. Zulauf, A biotechnological method provides access to aggregation competent monomeric Alzheimer's 1-42 residue amyloid peptide, Biotechnology (N Y) 13 (1995) 988-993.

[81] J. Busciglio, A. Lorenzo, and B. A. Yankner, Methodological variables in the assessment of beta amyloid neurotoxicity, Neurobiol Aging 13 (1992) 609-612.

[82] J. Davis-Salinas, and W. E. Van Nostrand, Amyloid beta-protein aggregation nullifies its pathologic properties in cultured cerebrovascular smooth muscle cells, J Biol Chem 270 (1995) 20887-

20890.

[83] A. Deshpande, E. Mina, C. Glabe, and J. Busciglio, Different conformations of amyloid beta induce neurotoxicity by distinct mechanisms in human cortical neurons, J Neurosci 26 (2006) 6011-6018.

[84] V. Rangachari, B. D. Moore, D. K. Reed, L. K. Sonoda, A. W. Bridges, E. Conboy, D. Hartigan, and T. L. Rosenberry, Amyloid-beta(1-42) Rapidly Forms Protofibrils and Oligomers by Distinct Pathways in Low Concentrations of Sodium Dodecylsulfate, Biochemistry (2007).

[85] M. Masuda, N. Suzuki, S. Taniguchi, T. Oikawa, T. Nonaka, T. Iwatsubo, S. Hisanaga, M. Goedert, and M. Hasegawa, Small molecule inhibitors of alpha-synuclein filament assembly, Biochemistry 45 (2006) 6085-6094.

[86] Y. Shimmyo, T. Kihara, A. Akaike, T. Niidome, and H. Sugimoto, Multifunction of myricetin on Abeta: Neuroprotection via a conformational change of Abeta and reduction of Abeta via the interference of secretases, J Neurosci Res (2007).

[87] X. R. Qin, H. Abe, and H. Nakanishi, NMR and CD studies on the interaction of Alzheimer beta-amyloid peptide (12-28) with beta-cyclodextrin, Biochem Biophys Res Commun 297 (2002) 1011-1015.

[88] B. Bohrmann, M. Adrian, J. Dubochet, P. Kuner, F. Muller, W. Huber, C. Nordstedt, and H. Dobeli, Self-assembly of beta-amyloid 42 is retarded by small molecular ligands at the stage of structural intermediates, J Struct Biol 130 (2000) 232-246.

[89] P. Friedhoff, A. Schneider, E. M. Mandelkow, and E. Mandelkow, Rapid assembly of Alzheimer-like paired helical filaments from microtubule-associated protein tau monitored by fluorescence in solution, Biochemistry 37 (1998) 10223-10230.

[90] S. R. Byeon, Y. J. Jin, S. J. Lim, J. H. Lee, K. H. Yoo, K. J. Shin, S. J. Oh, and D. J. Kim, Ferulic acid and benzothiazole dimer derivatives with high binding affinity to beta-amyloid fibrils, Bioorg Med Chem Lett 17 (2007) 4022-4025.

[91] C. Hetenyi, Z. Szabo, E. Klement, Z. Datki, T. Kortvelyesi, M. Zarandi, and B. Penke, Pentapeptide amides interfere with the aggregation of beta-amyloid peptide of Alzheimer's disease, Biochem Biophys Res Commun 292 (2002) 931-936.

VI. ACKNOWLDEGEMENTS

I would like to express wholehearted gratitude to my supervisor Prof. Il-Seon ParK for his guidance and continuous support to carry out this work. I would like to extend my sincere gratitude to my referee Professors, Kyung-Soo Hahm, Song Yub Shin, Eun-Rhan Woo and Byungyun Cho.

I am also indebted to my M.Sc. supervisor Prof. Achyut Prasad Sharma.

I like to thank my colleagues Giri, Pratap, Shahnawaz, Jung Eun, Sun-OH, Mi-hyun, Sun-young, Namting, Jung-Woo and Ju-Young.

Finally, I like to mention feel a deep sense of gratitude to my family members and kalu.

VI. ABBREVIATIONS

Ac-DEVD-AMC; *N*-acetyl Asp-Glu-Val-Asp-amino methyl coumarin

Ac-VDVAD-AMC; *N*-acetyl Val-Asp-Val-Ala-Asp-amino methyl coumarin

AKN; Adenylate kinase

AP; apigenin

Amento; amentoflavone

2',8''-biap; 2',8''-biapigenin

DTT; Dithiothreitol

FKBP; FK-506 binding protein

MALDI-TOF; matrix-assisted laser desorption-ionization-time of flight

MTT; 3-(4,5-dimethylthiazol-2yl) 2,5-diphenyl-tetarzolium bromide

NusA, transcription pausing factor L

RFU, relative fluorescence unit

SDS-PAGE, sodium dodecyl sulfate polyacrylamide gel electrophoresis

Suma; sumaflavone

TiG; trigger factor

TFA; 2,2,2-trifluoroacectic acid

Tricine; N-[2-hydroxy-1-bis (hydroxymethyl)] glycine

TF; taiwaniaflavone

VII. 적 요

아밀로이드 베타의 정제와

프라보노이드와의 상호작용기전연구

아르준 타파

지도교수: 박 일 선

조선대학교 대학원

생물신소재학과

원핵생물 체계에서 진핵생물의 펩타이드나 단백질의 발현은 종종 활성이 없는 봉입체 형태를 갖는다. 이러한 봉입체의 용해화와 제대로 된 구조를 만드는 과정들이 필요하며 여전히 어려운 작업이다. 이번 연구에서, 펩타이드와 단백질들이 용해되는 형태로 발현되는 효율적인 플라스미드 벡터 체계를 제작하였다. 발현시키고자 하는 뭉치는 경향이 있는 단백질이나 펩타이드를 용해화시킬 수 있는 융합 파트너를 붙이고, 이를 제거할 수 있도록 자를 수 있는 특정 부위를 넣어 원하는 단백질만 회수하는 방법으로 진행하였다. 융합 파트너를 찾기 위해 대장균에서 열에 안정한 단백질들을 선별하였고, 그들 중 높은 발현 효율과 안정성을 갖는 단백질을 확인하였다. 이를 이용하여, 봉입체 형태로 발현되는 아미로이드 베타(Aβ), 단백질, 펩타이들을 용해성을 갖는 형태로

발현하였고, 쉽게 분리할 수 있었다. 이러한 시스템은 뭉치는 형태의 단백질이나 펩타이드의 발현에 아주 편리한 방법을 제공할 것이다.

용해성 단량체 Aβ는 알쯔하이머의 주요 발병 인자로 간주되는 용해성 올리고머, 불용해성 섬유로 중합된다. 이번 연구에서, Aβ의 세포독성을 억제하는 작은 분자량의 물질을 부처손(*Selaginella tamariscina*) 식물로부터 분리하였다. 이 물질은 taiwaniaflavone(TF)로 확인되었고, staurosporine보다 Aβ42에 의한 세포사멸을 효율적으로 억제하였다. 원편광 이색성 분광분석기와 전자현미경을 이용하여 TF에 의한 Aβ 펩타이드의 구조적 변화 억제를 확인하였다. 더 나아가 thioflavin-T 결합 실험을 이용한 섬유생성 동역학 연구에 의해, TF 는 섬유생성과정에서 개시와 확장과정을 억제하는걸 확인하였다. 그러나, Aβ 올리고머의 축척은 Aβ섬유보다 더욱 독성이 강하다고 알려져 있다. 독성이 없어진 위의 결과들과 모순되게 보이나, TF가 Aβ 올리고머에 결합되어 있음으로써 약한 독성을 갖는 형태를 갖게 되고, 이에 세포독성이 사라지는 된 것이다. 실험의 모든 결과들은 TF가 독성이 있는 Aβ 종류들의 감소와 해독에 의해 Aβ의 독성으로부터 세포를 보호한 다는 것을 강력히 증명하고 있다. 또한, 다른 종류의 3가지 flavonoid (2',8''-biapigenin, amentoflavone, sumaflavone)들이 Aβ 올리고머의 형성과 세포독성에 있어서 비슷한 효과를 나타낸 반면에, 위 물질들의 단량체인 apigenin은 효과가 떨어지는 것을 확인하였다. 이러한 결과들에 의해, 많은 2량체 형태의 flavonoid들은 알쯔하이머 질환의 치료에 효과적일 것임을 예상할 수 있다.